

Article

Minute-Scale Forecasting of Wind Power - Results from the collaborative workshop of IEA Wind Task 32 and 36

Ines Würth ^{1*}, Laura Valldecabres ², Elliot Simon ³, Corinna Möhrlen ⁴, Bahri Uzunoğlu ⁵, Ciaran Gilbert ⁶, Gregor Giebel ³, David Schlipf ⁷, and Anton Kaifel ⁸

¹ Stuttgart Wind Energy, University of Stuttgart, Allmandring 5b, 70569 Stuttgart, Germany; wuerth@ifb.uni-stuttgart.de

² ForWind - University of Oldenburg, Institute of Physics, Küpkersweg 70, 26129 Oldenburg, Germany; laura.valldecabres@forwind.de

³ DTU Wind Energy (Risø Campus), Technical University of Denmark, Frederiksborgvej 399, 4000 Roskilde, Denmark; ellsim@dtu.dk, grgi@dtu.dk

⁴ WEPROG, Eschenweg 8, 71155 Altdorf/Böblingen, Germany, Willemoesgade 15B, 5610 Assens, Denmark; com@weprog.com

⁵ Dept. of Engineering Sciences, Division of Electricity, Uppsala University, The Ångström Laboratory, Box 534, 751 21 Uppsala, Sweden; Dept. of Mathematics, Florida State University, Tallahassee, FL, USA, 32310; bahriuzunoglu@computationalrenewables.com

⁶ Department of Electronic and Electrical Engineering, University of Strathclyde, 204 George St, Glasgow G11XW, UK; ciaran.gilbert@strath.ac.uk

⁷ Wind Energy Technology Institute, Hochschule Flensburg, Kanzleistraße 91–93, 24943 Flensburg, Germany; david.schlipf@hs-flensburg.de

⁸ Zentrum für Sonnenenergie- und Wasserstoff-Forschung Baden-Württemberg, Meitnerstraße 1, 70563 Stuttgart, Germany; anton.kaifel@zsw-bw.de

* Correspondence: wuerth@ifb.uni-stuttgart.de; Tel.: +49-711-685-68285

Academic Editor: Emanuele Ogliari, Sonia Leva

Version February 8, 2019 submitted to Energies

Abstract: The demand for minute-scale forecasts of wind power is continuously increasing with the growing penetration of renewable energy into the power grid, as grid operators need to ensure grid stability in the presence of variable power generation. For this reason, IEA Wind Tasks 32 and 36 together organized a workshop on “Very Short-Term Forecasting of Wind Power” in 2018 to discuss different approaches for the implementation of minute-scale forecasts into the power industry. IEA Wind is an international platform for the research community and industry. Task 32 tries to identify and mitigate barriers to the use of lidars in wind energy applications, while IEA Wind Task 36 focuses on improving the value of wind energy forecasts to the wind energy industry. The workshop identified three applications that need minute-scale forecasts: (1) wind turbine and wind farm control, (2) power grid balancing, (3) energy trading and ancillary services. The forecasting horizons for these applications range from around 1 second for turbine control to 60 minutes for energy market and grid control applications. The methods that can be applied to generate minute-scale forecasts rely on upstream data from remote sensing devices such as scanning lidars or radars, or are based on point measurements from met masts, turbines or profiling remote sensing devices. Upstream data needs to be propagated with advection models and point measurements can either be used in statistical time series models or assimilated into physical models. All methods have advantages but also shortcomings. The workshop’s main conclusions were that there is a need for further investigations into the minute-scale forecasting methods for different use cases, and a cross-disciplinary exchange of different method experts should be established. Additionally, more efforts should be directed towards enhancing quality and reliability of the input measurement data.

21 **Keywords:** wind energy; minute-scale forecasting; forecasting horizon; Doppler lidar; Doppler radar;
22 numerical weather prediction models

23 **1. Introduction**

24 In the past years, minute-scale forecasting of wind power has become an important research
25 topic in the wind energy community. Whereas traditional forecasting techniques provide a forecasting
26 horizon in the hour or day range [1], new methods allow to predict the power output of wind turbines
27 or wind farms on a minute scale. Due to the increasing penetration of renewable energy power systems
28 into the grid, there is a demand for minute-scale wind power forecasts, as grid operators need to
29 ensure grid stability in spite of the highly fluctuating power sources. The forecasts become even more
30 important with increasing sizes of wind farms of several 100 MW and especially if those wind farms
31 conglomerate geographically as is the case for offshore sites. The objective of this paper is to provide a
32 summary of the needs of minute-scale forecasting and an overview of the developed methods and the
33 possible solutions to the barriers that prevent end users from adopting them.

34 The results presented in this paper are based on the outcome of the collaborative IEA Wind Task
35 32 and 36 workshop “Very Short-Term Forecasting of Wind Power” held in Roskilde, Denmark in June
36 2018. IEA Wind Task 32: “Wind lidar Systems for Wind Energy Deployment” is an international open
37 platform with the objective of bringing together experts from the academic and industrial communities
38 to identify and mitigate barriers to the use of lidar for wind energy applications. IEA Wind Task 36:
39 “Forecasting of Wind Power” is focused on improving the value of wind energy forecasts to the wind
40 energy industry. During the workshop, 39 participants from academia, forecasting service providers,
41 wind farm operators as well as the lidar and wind turbine manufacturers discussed the future needs of
42 minute-scale forecasting, the advantages and barriers of different forecasting techniques and strategies
43 for overcoming those barriers.

44 This paper is organized as follows: Sections 2 and 3 discuss the need for minute-scale forecasting
45 and explain target forecasting horizons for different applications. In Section 4 state-of-the-art
46 forecasting methods and the need for new methods in the minute-scale is explained. Section 5
47 gives a review of methods for minute-scale forecasting. In Section 6 challenges for the implementation
48 and commercialization of the new methods are discussed and the paper is finalized with conclusions
49 in Section 7.

50 **2. Intra-hour variability of wind power generation**

51 In 2017 Denmark was the country with the highest wind power penetration rate (44% of the
52 annual consumption of electricity), followed by Portugal (24%) and Ireland (24%). In the case of
53 Denmark, the maximum hourly penetration rate was over 140%. With a total net installed capacity of
54 169 GW, the power generation capacity of wind power in Europe increased by almost 300% in the last
55 10 years [2]. Given the expected rising penetration levels of wind power and the increasing size of on-
56 and especially offshore wind farms feeding power into the grid at a single point [3], it becomes crucial
57 to have more precise forecasts of wind power generation with lead times of few minutes ahead and
58 temporal resolutions of seconds or minutes.

59 When generating a forecast, one useful practice is to consider the power spectral density (PSD)
60 of the measured physical process to understand which time frequencies contribute to the variance
61 of the signal. Peaks in the spectra correspond to larger relative fluctuations which are traditionally
62 more difficult to capture and predict. This type of analysis is demonstrated in Larsen et. al [4] using
63 long-term site measurements from Høvsøre test station and Horns Rev offshore wind farm in Denmark.
64 Boundary layer wind spectra were resolved across cycles ranging from 0.1 seconds (10 Hz) to 1 year.
65 Figure 1 presents a main result of that work which compares full scale wind PSDs at 50 m height both
66 on- and offshore [4]. Apt [5] presents a similar PSD analysis of wind turbine output using 1-second

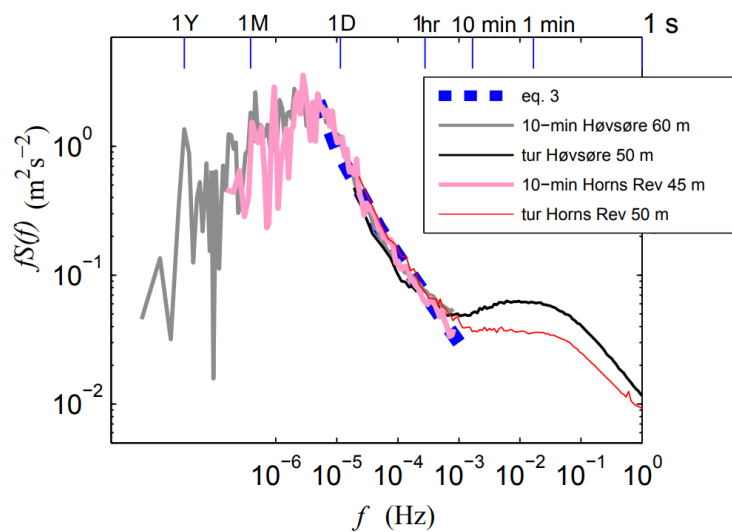


Figure 1. Power spectral density (PSD) of wind speed with corresponding timescales denoted atop. High frequency sonic measurements are used to devise the onshore (black) and offshore (red) lines. Reproduced with modifications from Larsen et. al [4] with permission from the Springer Nature publisher.

power data for a single wind turbine as well as a 6-turbine wind farm. Attributes of the PSD signal will vary by location, time, sensor type, and physical property being measured. Still, from the results in Figure 1, a strong local peak can be detected around 1 min, indicating the strong variability of the wind at that temporal scale. This variability of the wind is associated to atmospheric phenomena like open cellular convection, gravity waves, sea breezes or low level jets, among others [6]. At frequencies $f > 0.02$ Hz, i.e. periods below one minute, the PSD signal strongly decreases and, as reported in [7], wind power fluctuations of large wind farms are not considered an issue due to the smoothing effect of aggregated power.

Yet, the intra-hour variability of wind power not only depends on the variability of the wind itself but on the size of the wind farm, the number of wind turbines and their geographic dispersion. Indeed, it has been shown by several authors that for offshore wind farms, the small geographic dispersion of the wind turbines results in an increased power variability in the minute scale, compared to widely dispersed onshore wind turbines [8].

One of the main challenges for the integration of large amounts of wind power into the grid is the occurrence of rapid and strong changes in wind power generation (ramp events). These unexpected events are mainly caused by extreme changes in wind speed and/or direction in a very short period of time, and are frequently associated with the passage of weather fronts. However, the most critical ramp event can occur even for small changes in wind speed. When the wind speed reaches the wind turbine's cut-out speed, wind turbines shut down automatically for safety reasons, resulting in a large loss of generated power. Despite being critical for the management of the grid, the dynamic allocation of reserves and the stability of the system [9,10] there is no standard definition of a ramp event. It is an individual process of the end-user to define critical ramps and thereby ramp events. A recent publication on the history of wind power ramp forecasting [11] gives an overview of the definitions used in ramp event detection, the meteorological conditions associated to those events and the current forecasting techniques. For most wind power forecasting applications however, the definition of what is critical for an end-user is very individual and dependent on the application as well as the available reserves. For example, a system operator on an island grid or badly interconnected grid needs to have all reserves available within the control zone in order to prevent a critical ramp from causing security

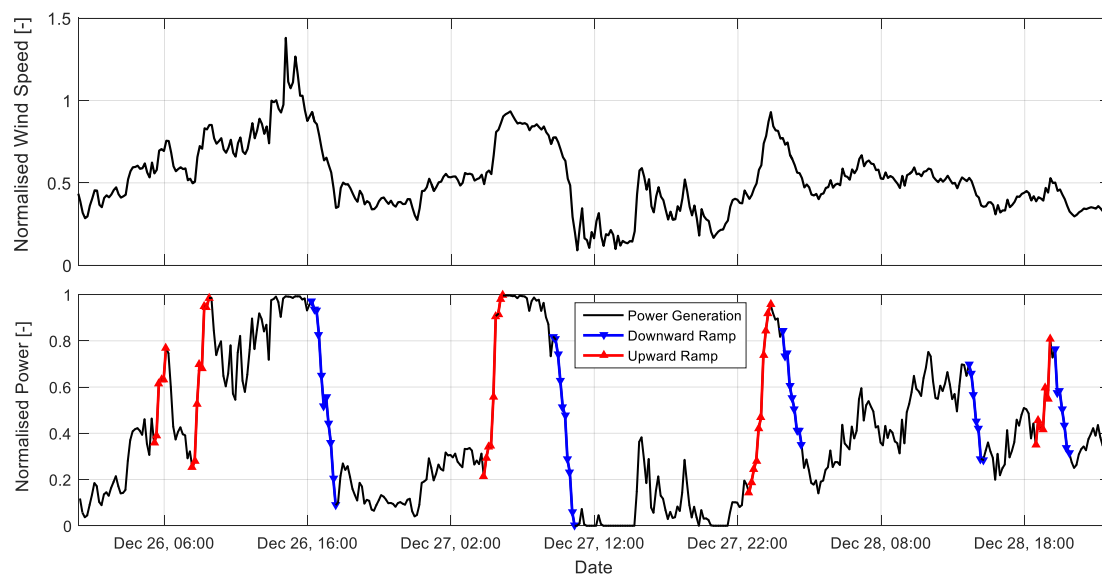


Figure 2. Example time series of wind speed and generated power of a single wind turbine with wind ramps marked for a time window of 60 min and a change of power of 40%. Each data point in the time series corresponds to a 10-minute average. Reproduced without modifications from Würth et al. [12] with permission <https://creativecommons.org/licenses/by/3.0/>.

issues. A trader may also be very interested in ramp forecasts, as just one event with a large error may cause 95% of the imbalance costs in a month.

Ramp events are often classified into ramp-up and ramp-down events, according to the direction of the power gradient. As an example, the time-series in Figure 2 illustrates a number of steep ramps in both directions. While ramp-up events can always be handled in the very short term with curtailments, ramp-down events can become extremely critical due to the sudden missing generation. This enhances the importance of generating accurate minute-scale forecasts of wind power.

3. An overview of different applications for minute-scale forecasting in the wind industry

The forecast horizon and the parameters that are needed to be forecasted depend on the application of the forecast. Three applications have been identified where minute-scale forecasts of wind speed or power are needed.

1. **Wind farm control:** Wind turbine and wind plant controllers need the information to optimize e.g. the power output of the turbines.
2. **Physical balancing:** They are required by the Transmission System Operator (TSO) in order to optimally operate reserves for the continuous balance of the power system and grid constraint management.
3. **Economic balancing:** Trading and balancing of wind power in the intra-day or rolling power markets require minute-scale updates of the forecasts with real power output in order to reduce imbalance costs and increase incomes.

It is expected that a next step in the evolution will be storage system planning and optimization in the real-time markets, where the bulk of the energy production will come from renewable energy sources. However, this paper focuses on the applications listed above. In the following each application is discussed in more detail.

Table 1. Helpful wind preview times for various wind turbine and wind farm applications.

Application	preview time
Single turbine blade pitch feedforward control	≈ 1 s
Single turbine model predictive control	≈ 10 s
Wind farm control via induction control	≈ 10 s to 10 min
Single turbine yaw control and wind farm control via wake steering	≈ 1 to 10 min

118 3.1. Wind turbine and wind farm control

119 Preview information of the wind field is helpful for the control of wind turbines and wind
 120 plants. Wind turbine and wind farm controller need to continuously adjust the operation of the
 121 controlled system due to the stochastic changes in the wind inflow. However, traditional controllers
 122 are mostly based on feedback and are only able to react to wind changes after the changes already
 123 have impacted the turbine dynamics and farm operation. lidar-assisted control algorithms can use the
 124 preview information of the wind to proactive adjust and thus improve the wind turbine and wind
 125 farm operation by increasing the energy production and reducing structural loads.

126 Regarding the required preview time for lidar-assisted wind turbine control, the following
 127 classification is useful:

- 128 1. around 1 s: Feedforward control is used to compensate wind changes to reduce structural loads.
 129 For e.g. the blade pitch, the rotor-effective wind speed is needed only a short time before the
 130 wind reaches the rotor to overcome the pitch actuator dynamics [13,14].
- 131 2. around 10 s: For Model Predictive Control, the control inputs are optimized to get a chosen
 132 compromise of load reduction, energy production, and actuator wear [15,16]. Here, a short time
 133 horizon of wind characteristics such as wind speed, direction, and shears is used, typical 5-10 s.
- 134 3. around 1-10 min: For yaw control, a wind direction estimation is used to align the wind turbine
 135 with the mean wind direction. Yaw control is generally done in the minute scale. In this time
 136 scale [17], the yaw signal of lidar systems provides good agreement [18,19].

137 Active wind farm control is a promising technology to increase the energy production of wind
 138 farms [20]. However, flow models are still an important research topic, and the validation of flow
 139 models and control strategies are still ongoing. Wind previews for flow control is mainly used in
 140 induction control and wake steering for higher energy capture and management of fatigue loading.

141 Regarding the required preview time for lidar-assisted wind farm control, following classification
 142 is useful:

- 143 1. around 10 sec to 10 min for induction control: Usually the blade pitch angle is used to reduce the
 144 power and thus the thrust to weaken wake effects on downstream turbines, which increase the
 145 overall production. At partial load this is done by adjusting the “fine pitch” settings which is
 146 usually based on a filtered wind speed estimate. Wind previews might help to better adjust the
 147 power balancing [21].
- 148 2. around 1-10 min for wake steering: The yaw misalignment is used to deflect wakes away from
 149 downstream turbines and thus similar preview times compared to the conventional yaw control
 150 is useful [22]. A preview of the wind direction might help to better adjust the yaw misalignment
 151 in a wind farm.

152 3.2. Power grid balancing, frequency control and power quality in reserve market

153 The focus in this section is on grid balancing, frequency control and power quality embedded in
 154 reserve market while the energy market and ancillary services are discussed in the following Section 3.3.
 155 The balancing term can be employed in a much broader sense in the context of balancing longer time
 156 scales. However in these time scales of mainly energy and reserve market, where balancing actions

Table 2. Activation of the reserves after an imbalance.

Application	Approximate range of operation	Overlap with other balancing
Primary control	≈ 0 to 2min	Transition overlaps secondary control
Secondary control	≈ 2min to 15min	Transition overlaps tertiary control
Tertiary control	≈ 15min to hour scales	

157 are scheduled before real time, there are several other means of observations with lower resolutions
 158 available. [23–25]. However, these are not within the time scales of minute-scale forecasting which is
 159 the focus of this section. It should be noted that there are differences in terminology between countries
 160 for the same and slightly different balancing actions. In this section, the EU terminology is adopted.

161 To guarantee the stability of the grid, supply and demand always have to be balanced in spite of
 162 the fluctuating power sources. Power quality is achieved if the grid frequency stays within a certain
 163 range of a rated value. An imbalance between supply and demand impacts voltage stability and grid
 164 frequency, hence there is a need for power balancing [23,26–28].

165 The volatility of wind resources creates volatility in the supply and as a result, balancing control
 166 actions are needed. One can distinguish between different time scales in this phase of controls
 167 embedded in the reserve market, which are known as primary, secondary, and tertiary controls. The
 168 autonomous response of the system to supply/demand imbalances is automatically addressed with
 169 primary controls, which is in the scale of microseconds to a few minutes mainly in the scale of seconds.
 170 In secondary controls, there are automatic actions and manual actions in scales of seconds to several
 171 minutes mainly in the scale of minutes. In tertiary control, both manual and automatic controls are in
 172 action from minutes to quarter of an hour to half an hour scales. These are summarized in Table 2. All
 173 of these actions of balancing are carried out in order to ensure power system quality.

174 From a market perspective primary, secondary and tertiary reserves are handled differently.
 175 Primary reserve is contracted on bi-lateral contracts due to the high-availability requirements.
 176 Secondary and tertiary reserves are in some countries traded by auction. The periods range from
 177 daily to several days or weeks. Common for all three reserve products is that the reimbursement is
 178 split up into a price for the availability of a specific generation capability and a price for the actual
 179 utilization [29].

180 Wind power and other renewable energy sources create low levels of rotational inertia since these
 181 energy conversion systems do not normally act on rotational inertia which has impacts on the power
 182 grid frequency. Moreover modern variable-speed turbines are disconnected by inverters from the
 183 rotating mass of inertia. Suppliers have started to make changes to create synthetic inertia that can
 184 emulate inertia synthetically [30]. Synthetic inertia is about acting to AC frequency, possibly after the
 185 loss of a big power plant which makes the grid under-supplied and will result with the AC frequency
 186 beginning to fall. This makes accurate short-term forecasting even more important since all of these
 187 emulations are dependent on accurate estimation of wind speeds. Hence automatic control for primary
 188 and/or secondary controls will certainly benefit from more accurate forecasting on the short-time
 189 scales of minutes in control applications.

190 On another note for the data that is available in the context of this research, any forecast data that
 191 is available on scale of microseconds to minutes can be automatically employed in the state estimator
 192 of the controller [23,26–28]. The state estimator corrects the state of the system with observational data.

193 3.3. Energy and ancillary services markets

194 Electricity markets need to be balanced in order to match the supply and demand of energy. This
 195 physical balancing of the transmission grid is carried out by the transmission system operators (TSO)
 196 or by an independent system operator (ISO). Given the increased integration of power generation from
 197 variable sources of energy like wind and solar, the physical balancing has become more complicated.
 198 Therefore, electricity markets with such intermittent and variable sources have to become more flexible

and introduce either rolling markets (e.g. in the UK and Australia) or introduce shorter intra-day auctions, additional to the day-ahead auction, which have become very popular in Europe. Among the intra-day market platforms, one can distinguish between discrete auctions or continuous intra-day markets. In intra-day auction markets like in Italy, Spain or Portugal, intra-day bids are restricted to a few established auctions. By contrast, in continuous intra-day markets, counter parties match the bids using a trading platform that operates continuously. Those continuous intra-day balancing markets operate in Europe with different lead times ranging from 5 to over 90 minutes and most of the countries work with trading blocks of 15 minutes. Table 3 includes the lead times and smallest trading blocks for several countries in Europe and for Turkey. A more detailed description of the electricity markets and their time lines can be found in [31]. Hence, the importance of the use of updated available minute-scale forecast of wind power has arrived to stay.

Table 3. Lead times and smallest trading blocks for different countries. Sources: EpeX [32], Nordpool [33], EXIST [34], and BSP South Pool [35].

Country	Lead time (minutes)	Trading blocks (minutes)	Market
Austria and Germany	5	15	EPEX Spot
Bulgaria, Denmark, Estonia, Finland, Lithuania, Norway and Sweden	60	15	NordPool
Belgium, France and the Netherlands	5	60	EPEX Spot
Slovenia	60	15	BSP Southpool
Switzerland	30	15	EPEX Spot
Turkey	90	60	EXIST

In light of this, the forecast process can be split into three components: (1) production of a smooth day-ahead forecast tuned for economic adjustment via the intra-day market, (2) targeting intra-day forecasts for the predictable part of the day-ahead forecast errors and (3) application of forecasts on the minute-scale to manage the wind power generation after gate closure of the intra-day. The two first components correspond to current practices in long-term and short-term processes with some enhancements. The third component is a process running on minute-scale with 1 or 2 hour look ahead [e.g. 36].

Minute-scale forecasts are also necessary when applying to provide ancillary services, secondary or tertiary reserve or balancing capacity for the pool of large utilities. For instance, a recent pilot project in Germany allows wind power generators to participate in the reserve market by down-regulating their production. The possible or available power produced by the wind farms needs to be calculated in one-minute intervals. Furthermore, the standard deviation of the percentage error of the possible or available wind farm power, during the pilot phase, should be less than 5% [37].

4. State-of-the-art of wind power forecasting

State-of-the-art wind power forecasting methodologies utilize wind speeds from weather forecasts and on-site real-time measurements to compute wind power.

Figure 3 shows qualitatively the forecast error levels of a day-ahead, hours-ahead and minutes-ahead forecast compared to a persistence error, where the persistence forecast is the most recent available measurement. The qualitative visualization of the forecast errors in the different time scales shall be seen in the light of their starting point and forecast error growth over time. For example the day-ahead forecast has an almost linear error growth and is typically responsible for approximately 1/3 of the forecast error [38]. The day-ahead forecast also starts with an inherent error at forecast time zero due to a number of aspects. In [38] these are described as for example (i) the initial weather conditions; (ii) sub grid scale weather activity; (iii) coordinate transformations; (iv) the algorithm used to compute the wind power; (v) imperfection of turbines and measurement errors. For Pahlow et al. [38] one question remained: which fraction of this background error is caused by

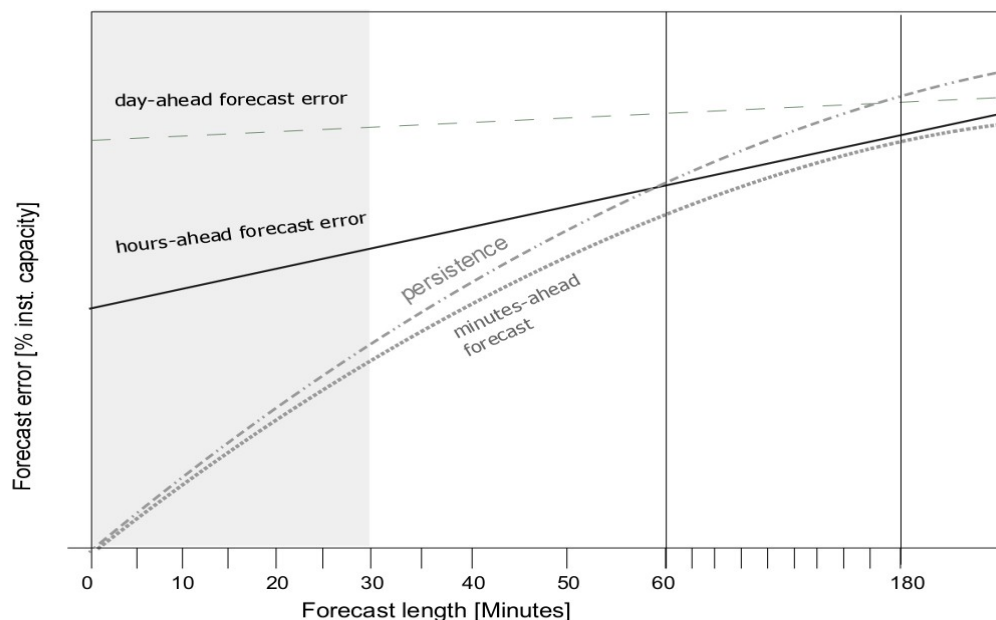


Figure 3. Qualitative visualisation of the forecast error development over the first hours of a forecast for different temporal forecast techniques.

imperfect initial conditions of the weather forecast and which fraction is due to erroneous wind power parameterizations. They extrapolated the linear forecast error growth from 9–45 hours down to the 0 hour forecast and thereby estimated the background mean absolute error (MAE) just under 4% of installed capacity. Part of that gap of approximately 4% error at the initial time can be reduced by the hours-ahead forecast with knowledge about the real power production. Pahlow et al. [38] characterized this inherent error at the initial time to a mix of unknown technical and non-technical constraints at the forecast location. These can be wind farm specific constraints, such as unknown non-availability of wind turbines, but also errors due to the computation of the wind power at the site. The hours-ahead forecasts are steeper in error growth than the day-ahead and reach this level typically around 4–8 hours ahead in time. This time span is the typical temporal influence radius of a measurement [38]. The minute-scale and persistence forecasts are both starting at the zero error in their initialization. This is what characterizes this forecasting time scale, where the current state of the power plant is fully known. The steepness of the error is also highest for these two forecast techniques due to the decreasing influence of the measurement at the power plant over time. A general industry experience is that a persistence forecast is at the same level as a hour-ahead forecast after around one hour. A minute-ahead forecast should ideally be below the hour-ahead forecast for about 3 hours as a thumb rule when evaluating the usefulness of the technique. The time between 1 hour and 3 hours into the forecast is where the persistence forecast typically reaches the day-ahead forecast error level and loses forecast skill.

Figure 3 illustrated nicely that the margin of possible improvements by minutes-ahead forecasts in the first 30 minutes of the forecast is rather small in comparison to persistence. Additionally, the average error growth of up to 2% of the installed capacity of a short-term forecast of 15 minute time resolution is rather steep (see Figure 3). It is therefore fair to say that the improvement over persistence, which is the objective in the very short time ranges of minutes and hours, is therefore rather modest. This is often used as a reason not to base decisions on forecasts, but rather use persistence, even during ramping, where the persistence forecast is a poor approximation. If the previous 15-minute forecast already appears to be off track, then the forecast user cannot be justified in trusting the forecast. Also,

263 the similarity between the average error of a short-term forecast and persistence over the next 15
264 minutes strongly indicates whether the short-term forecast performs better or worse than persistence.

265 Forecast providers are continuously looking for enhancements, which can improve the hour-ahead
266 and minute-scale forecast in the less good quality periods, because these result in the most significant
267 power system benefits. Use of wind speed measurements in addition to wind power measurements is
268 therefore a key to improve forecasts in periods, where the wind speed is in the flat ranges of the power
269 curve ($< 5 \text{ m/s}$ or $> 12 \text{ m/s}$). Without wind speed measurements, the minute-scale forecast is in fact
270 unable to correct the weather forecast for phase errors in periods, where the generation is zero or at
271 full capacity.

272 A forecast of the steady increase in wind speed from 15 m/s to above the high-speed shutdown
273 point at 25 m/s can also be improved by using wind speed measurements in short-term algorithms. At
274 the high-speed shutdown points ($> 25 \text{ m/s}$), the wind speed forecast uncertainty is at least 2 m/s even
275 in highly predictable events. The timing of the shutdown is therefore uncertain, even a few minutes
276 before it happens. Wind speed measurements from wind farms reduce this uncertainty significantly.
277 The timing of a high speed shutdown is important for grid security, because there are potentially many
278 Megawatts instantly ramping down. In combination with forecasting on the minute-scale, such wind
279 speed measurements can help to bridge the gap between actual generation and both short-term and
280 long-term forecast.

281 For wind speeds below the cut-in level there are similar considerations. Mostly, low aggregated
282 wind power generation occurs at low wind speeds. Nevertheless, a large and strong low pressure
283 centre may have near-zero wind speeds from different directions. Both the changes in wind direction
284 and wind speed are better identified by wind speed measurements than wind power measurements.
285 Thus information about wind speeds below cut-in can be crucial for the forecast accuracy near a low
286 pressure system center with highly aggregated wind power generation. During periods of moderate
287 and high generation, wind speed measurements can be used to calculate current potential turbine
288 available generation power or validate the signal of current available power generation sent by the
289 wind generation plant. To conclude, measurements of low, medium and high wind speeds all add value
290 to forecasting, while measurement signals in the steep range of the power curve are least important.

291 From a technical perspective of the instrumentation, one of the most reported gaps for forecasting
292 hours-ahead and minutes-ahead is the quality of the measurement signals. While wind farm developers
293 have to use calibrated instrumentation and standardized methodologies in order to obtain a bankable
294 level of siting accuracy in the first planning and commissioning phase of a wind project, in the following
295 operational phase the use of meteorological measurements is mostly not defined, documented or
296 standardized. Although the measurements are important in many ways, e.g. situational awareness in
297 extreme events, scheduling and dispatch of generation on power system level, the balancing of large
298 forecast errors, maintenance of instrumentation, there are no standards for the quality of the signals
299 in real-time environments today. For example, if a measurement stops working correctly and sends
300 constant values, a persistence forecast that uses only this data will benefit in performance assessment,
301 while a more advanced minute-ahead forecast that uses other data or models is penalized for providing
302 a more realistic view of the situation. Dependent on the amount of such periods with constant values,
303 this can easily lead to an overestimation of the performance of a persistence forecast in comparison to
304 minutes-ahead forecasts and thereby prevent use and application of minutes-ahead forecasts.

305 Due to such missing standards and industry guidelines, the main gaps for the use of and collection
306 of meteorological measurements and thereby advances in minute-scale forecasting can be summarized
307 as:

- 308 • lack of requirements in the grid codes
309 • lack of strategy for handling of missing or constant signals from measurements in real-time
310 • lack of quality of measurements in real-time

311 5. Review of methods for minute-scale forecasting

312 In the previous section we discussed the state-of-the-art in minute-scale forecasting. In this section
313 we investigate instrumentation that can improve forecasting with current techniques and we outline
314 which and how new types of instrumentation and models can be used to improve forecasting on
315 minute scales when persistence can no longer provide a correct picture of the weather conditions.

316 5.1. Minute-scale forecasting based on preview data from remote sensing devices

317 Remote sensing techniques are a new technology development in wind energy applications,
318 which have their roots in the desire to find alternative measurements for the expensive and at times
319 difficult installation of meteorological masts. With increasing experience and technical advances in
320 technology, remote sensing devices have become viable alternatives. This has also been reflected in the
321 IEC 61400-12-1 2017 standard [39], where such devices have been incorporated as possible instruments
322 to carry out measurements for wind energy applications. A new application for remote sensing
323 devices is forecasting. Especially scanning devices such as scanning lidars and radars which offer
324 the possibility to carry out minute-scale forecasts by delivering high resolution temporal and spacial
325 previews of the upstream wind field of a wind turbine or wind farm. Therefore, the next subsections
326 give an overview of using those devices for forecasting purposes and finally lessons learned with
327 remote sensing instruments in real-time forecasting projects are summarized.

328 5.1.1. Scanning lidar-based propagation models

329 Doppler wind lidars measure the wind speed in direction of the laser beam, also referred to as
330 line of sight (LOS). Depending on the system, the measurement range varies from a few centimeters
331 to several kilometers [40]. Commercial lidars were first used for wind energy applications in the
332 early years of this millennium [41]. Nowadays they have become accepted as an alternative to
333 meteorological masts (met masts) due to cost and ease of installation. Ground based systems are used
334 for site assessment and power performance testing and are now included in international standards
335 [39]. Nacelle-based lidars that can measure upstream of operating turbines, are used for feed-forward
336 control of wind turbines [42]. These systems measure the wind speed several hundred meters upwind,
337 thus forecasting the rotor effective wind speed seconds before it hits the rotor just in time to pitch
338 the rotor blades and reduce loads. A new application for scanning lidars is within wind power
339 forecasting. Commercial lidar manufacturers have increased the range of their systems and compact
340 pulsed scanning wind lidars may now measure the wind speed up to a distance of 10 km over an
341 entire site from one location [see e.g., 43,44]. There are also systems on the market that measure 30 km
342 and more, but these systems are bigger in size and therefore less suitable for flexible measurement
343 campaigns. The basic idea is to use the spatial and temporal high resolution wind field information
344 measured several kilometers upwind of a wind turbine or wind farm to forecast the power output
345 ahead in time.

346 The forecast process (Figure 4) is the same for both applications – control and power grid balancing.
347 First the raw lidar data is filtered and the horizontal wind speed and direction is reconstructed from the
348 measured LOS wind speeds. Depending on the number of synchronized lidar measurements, different
349 assumptions need to be made in order to resolve both horizontal wind speed and direction. For
350 instance, a velocity-azimuth display (VAD) retrieval technique is used to resolve both wind speed and
351 direction when only one lidar measurement is available [45]. This method assumes a homogeneous
352 wind field and should only be used in flat terrain where the assumption generally holds true. Then
353 the wind speed in the distance is propagated towards the site by means of a propagation model. The
354 simplest model is based on Taylor's hypothesis which claims that turbulent structures, so called eddies,
355 are transported with the mean flow without changing their properties. With this assumption the time
356 can be calculated that the wind speed measured in a certain distance needs to reach the turbine or
357 wind farm. Thus the farthest measured distance determines the forecast horizon. The forecasted wind

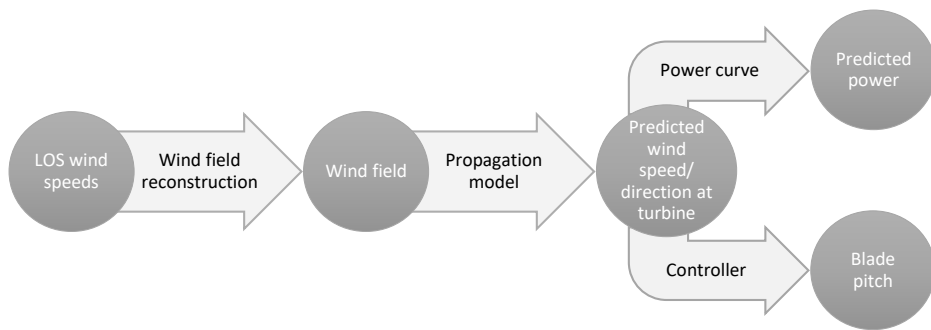


Figure 4. Forecast process using scanning lidar data.

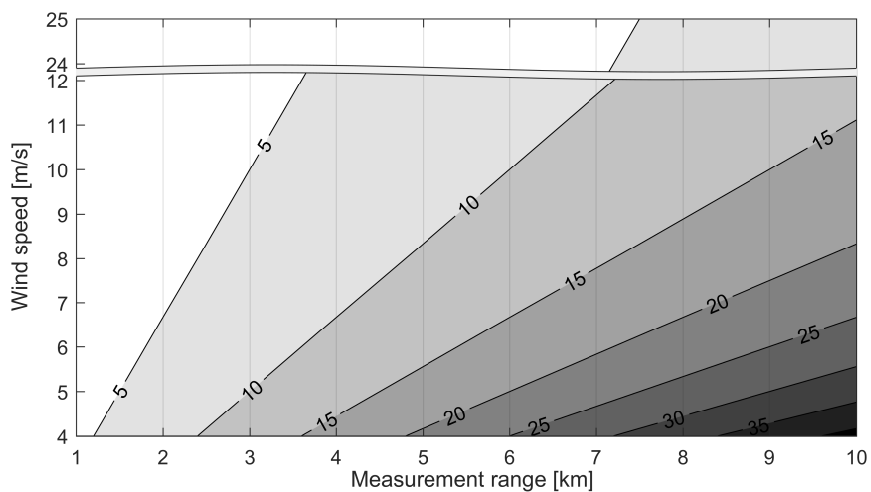


Figure 5. Forecast- horizon calculated based on Taylor for different wind speeds and measurement ranges; the horizon is given in minutes.

358 speed at the turbine or farm location is then used either to forecast the power output by means of a
 359 power curve model, or as an input to the wind turbine controller.

360 As mentioned, the forecast horizon is determined by the measurement distance of the lidar and
 361 the magnitude of the wind speed (Figure 5). For wind speeds at rated power of a typical turbine, the
 362 maximum forecast horizon with a state-of-the-art long-range scanning lidar that ideally measures up
 363 to 10 km is around 15 min. The maximum horizon increases to around 40 minutes for a wind speed of
 364 4 m/s that corresponds to a typical cut-in wind speed.

365 The advantage of scanning lidars is that they offer the possibility to directly measure the wind
 366 speed upstream of a turbine. All long-range scanning lidars are pulsed devices, which means that
 367 the wind speed information is gathered simultaneously at different measurement distances. Thus
 368 the wind flow can be tracked over the span of the measurement and local changes in the wind speed
 369 are captured. Modern lidars have compact dimensions of around one cubic meter which allows for
 370 flexible measurement campaigns and the installation for instance on the nacelle of a wind turbine or
 371 other elevated points such as an offshore substation. Then the scanning of the area on e.g. a horizontal
 372 arc leads to the desired horizontal wind speed information after reconstruction without having to
 373 take into account shear effects. When installing the lidar on the nacelle of a wind turbine behind the
 374 rotor, it should be noted that due to the blade passage the available data will be reduced, and nacelle
 375 vibrations and the tilt angle from the rotor thrust might introduce disturbances in the measurement
 376 range and height.

Recent investigations have shown that lidar-based forecasting models were able to predict near-coastal winds better than the benchmarks persistence and ARIMA for a forecasting horizon of 5 min [46]. Another relevant study is Simon et al. (2018) [47] which explores space-time correlations of upwind lidar observations measured on a flat horizontal plane. The study also shows results of a 1-60 minutes ahead forecast method utilizing the lidar inflow scans which significantly outperforms the persistence method.

However, there are some drawbacks when using lidar data for forecasting. One of the major barriers to overcome is the availability of the measurements. The lidar measures the wind speed by sending out laser pulsed that are backscattered from particles suspended in the air. The wavelength of the backscattered light shifts relative to the speed of the aerosols according to the Doppler principle [48]. Therefore the device records a noisy signal if not enough or too many aerosols are in the air. It also means that the measurement range fluctuates due to environmental conditions such as fog or rain showers [49]. And as the measurement range determines the forecast horizon, minute-scale forecasts are not possible if the lidar is blind. As a consequence, a fallback solution should be implemented in case the lidar does not provide measurements. Data from other sensors such as radar or drone measurements could be one solution. Using statistical models (cf. Section 5.2) or the coupling of the measurements with NWP models (cf. Section 5.3) could be another solution. More investigations have to be carried out to determine the optimum conditions for good range measurements of lidars.

Another drawback of lidars so far have been the high costs and the inaccuracies of wind field reconstruction in complex terrain. According to the white paper of the Deutsche Windguard [50] and [51], especially “in complex terrain sites, influence of the relatively large scanning volume of today’s lidar and SODAR must be carefully considered in terms of its influence on the measurement accuracy...”. This has been a general observation and an ongoing research topic [see e.g., 52–57]. In one recent large scale measurement campaign, the Land-Atmosphere Feedback Experiment (LAFE), measurements were setup with multiple synchronized scanning lidars that enable the direct measurements of wind field components [see e.g., 58,59]. Their instrument setup configuration addressed “the required combination of measurements for advanced studies of the land-atmosphere feedback” with a combination of instrumentation of scanning lidars and surface and airborne in situ measurements that provided the necessary overlap of measured data signals to fill gaps in the instrument’s measurement ranges. This strategy could directly be transferred to the minute-scale forecasting problem in real-time environments and in complex terrain and is also widely applied in the data assimilation of NWP models (see section 5.3).

Another significant obstacle for the application of lidars in the wind power industry is the lack of standard or recommended practices for the use of scanning lidars for wind speed forecasting. More research is needed to find out what the ideal measurement setup looks like, in particular how many lidars are needed and where to place those devices within a wind farm or within a control zone of a system operator. Also, optimal measurement strategies need to be established and transferred to different problem areas and sizes. To that end, different use cases have to be investigated to find out what the best campaign setup and measurement strategy is. Such use cases should include on- and off-shore wind farms of different scales. Recommended practices then need to be consolidated so that the widespread use of lidar for forecasting becomes possible on a commercial level.

5.1.2. Radar-based density models

Radar are remote sensing systems which can determine the position, angle or motion of objects and are being used in multiple applications including traffic control, ocean surveillance, weather monitoring, flight control systems and antimissile systems. Similarly to wind lidars, Doppler radars can be used for wind power forecasting as they are able to determine the velocity of the objects. The working principle is the same as for lidars, but rather than sending light waves, they emit radio waves. Thus, in an environment where meteorological particles with high humidity such as water droplets or

425 ice crystals are present, radars are able to measure the wind speed by determining the motion of the
426 hit particles.

427 The maximum range that radars can measure is given by the wavelength of the signal emitted, but
428 in this paper we only focus on radars which work on wavelengths that are of interest for minute-scale
429 forecasting of wind power. Thus, we limit our review to radars working between the C-Band and the
430 Ka-band radars, or with a wavelength of 3.2 cm to 8.6 mm.

431 Doppler-radars working in the Ka-band (35 GHz) are optimal candidates for wind power
432 forecasting (Figure 6). The short wavelength employed allows for high temporal and spatial resolution
433 of the measured wind fields. As with lidars, Doppler radars measure the LOS wind speed. Thus,
434 measuring with one Doppler radar over a defined Plan Position Indicator (PPI) trajectory, the horizontal
435 wind speed can be determined by applying a VAD retrieval technique in the same manner as lidar.
436 To derive the two horizontal wind speed components, two synchronized Doppler radars are needed
437 [60]. The number of publications on the use of Doppler radars for wind energy applications has grown
438 in the last years. Hirth et al. coupled wind farm operational data with wind fields measured by two
439 synchronized Doppler radars (dual-Doppler radar) to further investigate wind farm wake effects [61].
440 Dual-Doppler measurements of the wake behind an offshore wind farm were also reported by Nygaard
441 et al. [62]. The performance of wind turbines was also validated with dual-Doppler measurements in
442 [63].

443 First evidence of the promising application of Doppler radar systems for forecasting purposes was
444 documented by Hirth et al. [64]. An extreme wind ramp event observed by the Texas Tech University
445 Ka-band radars at a wind farm in Oklahoma was presented. The authors merged dual-Doppler wind
446 fields with operational data from 32 wind turbines to document the observed transient wind event
447 and its effect on the wind turbines' performance. They also coupled data from a meteorological tower
448 to analyze the weather conditions that originated the transient event.

449 Recently, it was shown that Doppler radar observations can be employed to derive minute-scale
450 density forecasts of wind power. In [65] the authors proposed a methodology that uses dual-Doppler
451 radar observations of wind speed and direction in front of a wind turbine to forecast the power
452 generated in a probabilistic framework. In a case study, they predicted the power generated by seven
453 turbines "free-wake" wind turbines in an offshore wind farm. Predictions were generated with a
454 temporal resolution of one minute and with a lead time of five minutes. With their study, the authors
455 showed that the radar-based forecasting model is able to outperform the persistence and climatology
456 benchmarks in terms of overall forecasting skill and generate reliable density forecasts in the case of
457 optimized trajectories.

458 One of the main advantages of Doppler radars is the extended range they can measure (over
459 30 km). Additionally, the optimal trade-off between the temporal (one minute) and spatial (50 m)
460 resolution of dual-Doppler radar measurements, compared to that of typical wind measurements from
461 met masts or satellites, makes them promising candidates for minute-scale forecasting of wind power.
462 As with lidars, the same wind power forecasting process can be implemented to derive a wind power
463 forecast. Besides, the fact that they can perform volumetric measurements (wind field measurements
464 at multiple heights), allows to infer further information such as horizontal and vertical wind shear.

465 However, as with lidars, one of the main obstacles to the adoption of radar as a forecasting tool
466 is the availability of the measurements. The radar measurement principle lies in the backscattering
467 of particles in the air containing high humidity such as water droplets or ice crystals. Therefore, the
468 quality of the measurements relies on the concentration of these particles in the air [60]. Besides, the
469 relatively large dimensions of Doppler radars complicate their installation and reduces the range of
470 possibilities for placing them, especially in offshore environments. The advantage of Doppler radar
471 with respect to lidars is the maximum range that they can measure. However, compared to lidars, the
472 wider beam width of radar results in larger beam spread at large ranges.



Figure 6. One of the two Doppler radar units deployed for the BEACON project [62,65].

473 5.1.3. Weather radars for prediction of strong wind power fluctuations

474 Although we have mainly focused on the use of Doppler radars for forecasting applications,
475 weather radars have been also identified as promising candidates for very short-term power forecasting
476 of offshore wind power. Modern weather radars working in the C and X-band measure the intensity
477 of precipitation. They are, consequently, able to anticipate precipitation fields associated with severe
478 wind speed and power fluctuations. The capabilities of anticipating strong wind power fluctuations in
479 offshore wind farms using local weather radars was introduced in [66,67]. In their work the authors
480 were able to track the arrival of precipitation events to the surroundings of an offshore wind farm. These
481 events were highly correlated with the strong observed power fluctuations. The authors also identified
482 shortcomings of the use of weather radars for wind power forecasting, which included: interception of
483 radar waves (cluttering), beam attenuation due to intense precipitation, anomalous propagation of
484 the radar waves during specific atmospheric conditions, underestimation of precipitation reflectivity
485 (beam filling) during convective events, and overshooting at long ranges due to the curvature of the
486 Earth.

487 5.1.4. Lessons learned with remote sensing instruments in minute-scale forecasting projects

488 Several research projects have been conducted with the goal of integrating remote sensing
489 measurement into real-time forecasting projects. For this purpose not only were scanning devices
490 deployed, but also ground-based profiling devices. In the largest and longest measurement campaigns
491 targeted towards real-time forecasting of wind energy in recent years were two projects funded by
492 the United States Department of Energy. In the Wind Forecasting Improvement Project (WFIP I and
493 II) [68] there were 12 wind profiling radars, 13 sodars and three lidars amongst other meteorological
494 sensors used. Lidars as well as sodars are basic equipment used in meteorological data assimilation
495 today and have been quality checked following meteorological standards through the Meteorological
496 Assimilation Data Ingest System (MADIS) [69]. This was a necessary step in order to integrate the
497 simulations into real-time model forecast systems [70]. In the second project, “Distributed Resource
498 Energy Analysis and Management System (DREAMS) Development for Real-time Grid”, a number of
499 sodars and lidars were used to enhance the Hawaiian system operator’s EMS (Energy Management

500 System) tools for situational awareness of critical events [71]. Here, the instruments were used for the
501 first time as part of an operational management system at a system operator in real-time.

502 From the above described studies and experimental measuring campaigns as well as real-time
503 testing it can be concluded that remote sensing instruments need to be serviced and maintained
504 similarly to any other real-time instrument. Skilled personnel are required in order for the the devices
505 to run continuously and reliably.

506 The following list presents the major findings and recommended technical requirements from
507 these studies and real-tiem tests towards ensuring high quality data during long-term real-time
508 operation:

- 509 • Lightning protection and recovery strategy after lightning should be ensured.
- 510 • Instruments must be serviced and maintained by skilled staff.
- 511 • Version control must be maintained for signal processing.
- 512 • Measurements must be the originally measured values or technical requirements must include
513 maintenance and software updates.
- 514 • Wind data should be measured at a height appropriate for the wind farm, either at hub height or
515 preferable at both hub height and the lowest possible measuring height (e.g. 30 m).
- 516 • Remote sensing devices in complex terrain require special consideration.

517 From studied projects and measurement campaigns, it can be concluded that in active weather
518 conditions, i.e. at the flat range of the power curve as well as under strong precipitation events, it
519 must be expected that met-mast anemometers are more reliable than sodar or lidar devices. From a
520 forecasting and operational monitoring perspective, conditions outside of the instrument's operating
521 conditions are some of the most critical conditions for grid operation, such as storms with precipitation
522 or high winds. Sodars are more prone to data delivery failures than lidar. In general, however both
523 devices suffer under non accessibility of measurement information in - for the grid operator - critical
524 situations.

525 5.2. Statistical time series models

526 Statistical approaches to forecasting problems mainly rely on deducing patterns from past
527 observational data and extrapolating these relationships to predict future values over a desired
528 time step. With wind energy applications in mind, in this section we consider the task of forecasting
529 a one dimensional time series signal such as a wind speed measurement, or a SCADA source such
530 as wind turbine or wind farm active power signal. The chosen forecast horizon should relate to
531 the time resolution of available input data, and at minimum be one sample (time step) ahead to
532 avoid errors introduced by interpolation. Statistical forecasting methods used on the minute scale are
533 largely identical to techniques employed for longer horizons. The main differences being the temporal
534 resolution of the data and the variability of the physical process being predicted (see Section 2).

535 Data acquisition systems are ordinarily capable of sampling and saving data at high frequency,
536 although historically this data has not always been used nor recorded. For the purposes of minute-scale
537 forecasting, 10-minute or hourly averaged data sets are not sufficient for capturing signal characteristics
538 needed to construct and validate a well performing statistical model. For this reason we recommend
539 that all data generators ensure that they have access to and are logging their high frequency data (both
540 turbine and meteorological sources), and that the instruments are properly maintained. The lower
541 bound of the recorded sampling rate should be at minimum twice the highest frequency in the analog
542 signal you wish to capture, in order to avoid aliasing in the discrete signal transformation (Nyquist
543 sampling theorem). In practice, 1 Hz (1 sample per second) is proposed as a compromise between
544 functionality and transmission/storage considerations. This will allow for future model building and
545 testing which can resolve fluctuations on the minute-scale.

546 Time series data contrasts to cross-sectional data in that it is naturally ordered in time. Samples
547 which are closer together will normally express a higher correlation than those further apart. This

548 temporal link should be explored through inspection of the autocorrelation and partial autocorrelation
549 function of the time series before beginning any attempts to build a model.

550 There are often a number of characteristic sub-components embedded in the time series which can
551 be obtained through decomposition techniques in order to normalise samples across time. Examples
552 include differencing an integrated series, removing an overall trend (usually by either mean subtraction
553 or model fitting to obtain the residuals), accounting for cyclic fluctuations, and adjusting for seasonal
554 variations.

555 A common assumption made by statistical forecasting methods is that of stationarity. Stationary
556 processes comprise of data where the mean, variance, and autocorrelation structure do not change over
557 time. By implementing the techniques described above, it is possible to transform a non-stationary
558 time series into a stationary one which can be used with traditional forecasting methods.

559 Benchmarking in any forecasting exercise is crucial. Commonly for forecasting at these short
560 timescales the persistence and climatology models are employed; these simple methods assume that
561 the forecast for the target variable is the most recent available measurement or summary statistics of
562 historical measurements, respectively. Statistical methods for wind speed and power forecasting are
563 typically based on time-series models such as autoregressive [72] (AR) and autoregressive moving
564 average (ARMA) [73,74] models as well as other soft computing techniques such as neural networks
565 [75].

566 Purely AR models are formulated as a weighted combination of past observations (lags) where the
567 coefficients are normally estimated via ordinary least squares regression. The order of the AR model,
568 or maximum lag, is crucial and can be chosen most simply by inspection of the auto-correlation and
569 partial auto-correlation functions of the signal. Cross-validation or an information criterion provide
570 an alternative method for defining the model order. Domain knowledge of the local meteorological
571 conditions can also be used to extend these simple models. For example, in certain regions the
572 wind/power time series may exhibit strong diurnal trends which would necessitate the inclusion of
573 time-of-day into the model.

574 Beyond time series models, machine learning techniques also are widely employed. These
575 techniques can be more flexible than classic time series models in terms of easily allowing for more
576 explanatory variables and are typically more naturally able to capture non-linear relationships. It
577 should be noted that this comes at the expense of additional model tuning to optimize algorithm specific
578 hyper-parameters and possible overfitting of the data unless careful cross-validation procedures are
579 followed. Examples include artificial neural networks [75], hybrid multi-models with blending [76]
580 together with feature selection [77], and penalized regression [78].

581 Artificial neural networks, particularly recurrent neural networks (RNN), have been widely
582 applied for sequence prediction including time-series data. Long short-term memory (LSTM) networks
583 are explicitly designed to capture data patterns of arbitrary lags, and assimilate long-term temporal
584 dependencies [79]. This has led to numerous applications in energy forecasting which outperform
585 traditional time-series modeling approaches. Wu et al. [80] demonstrates such a probabilistic 4-hour
586 ahead wind power forecast employing a LSTM network architecture.

587 Statistical forecasting models can also be made dependent on the current behaviour of the target
588 time-series or on exogenous variable(s). These are termed regime-switching models and can be based
589 on unobserved regimes [81,82] or by observed regimes like atmospheric conditions [83,84]. It follows
590 that these regimes can be derived from lidar/radar measurements [67]. The benefit of regime switching
591 is that the statistical models can react faster to changing conditions, as opposed to having a fixed
592 coefficient models or by tracking slower changes in behaviour via for instance an online update of the
593 coefficient estimates.

594 Concurrent information from spatially distributed wind farm or met mast measurements also
595 provide a route for improvements in forecast skill [85,85]. Multivariate forecasts which encode
596 information on the spatio-temporal dependency of neighbouring sites can be tackled via a vector
597 autoregressive models (VAR) at these time horizons. With an increasing number of sites, making

598 sparse estimates of the coefficient matrices becomes more important, as does estimating them via
599 efficient numerical procedures [86–88].

600 Forecast uncertainty at these horizons can also be accounted for via probabilistic density forecasts,
601 quantiles, or prediction intervals [89]. These may be generated using parametric assumptions of the
602 forecast distribution shape [72] [90] or non-parametric techniques [91] [92]. Uncertainty forecasts
603 enable the user to manage risk in decision making and leverage more actionable information from
604 their data, if information content is communicated properly [93].

605 These discussed statistical methods have been widely proven to increase forecast skill over
606 persistence at time-horizons generally at a minimum of 10 minutes ahead. Further research is required
607 to evaluate the suitability of statistical methods below this time horizon and at what time range
608 forward facing lidar/radar based systems or hybrid statistical and radar/lidar systems are a more
609 suitable choice.

610 5.3. Statistical data assimilation based on physical models

611 Data assimilation performs an essential role in the forecasts of wind power systems. While the
612 concept is very inclusive, meaning assimilation of any data with any model, in this section, the term is
613 used in more exclusive sense without addressing statistical time series models. Time series models are
614 a special case of data assimilation where usually non-physical models are taken into consideration.
615 This was discussed in the previous section. The concept is inherent from the fact that neither the model
616 nor the observations are perfect. In order to have an accurate state of the system, the numerical model
617 itself is not sufficient and therefore guidance from observations is required. This is even more so for
618 weather forecast systems, where the system itself is very sensitive to initial conditions and boundary
619 conditions. Data assimilation was first employed in engineering, however today it is more than an
620 engineering tool.

621 In summary, in the context of this review article, data assimilation is a technique to adopt multiple
622 measurements and observations of different types into a 3-dimensional model space. In meteorology it
623 is used to generate an initial state of the atmosphere from observations, i.e. an input field, together
624 with boundary conditions to any numerical weather prediction (NWP) model.

625 Also for the renewable energy production, data assimilation and/or state estimation has an
626 important role, for example in the assimilation of data into the control system on wind turbine or even
627 wind farm level. System operators and wind farm operators require advanced knowledge of ramp-up
628 and ramp-down events [94–96]. In a ramp/extreme event forecasting you want to analyze and use
629 outliers in order to assess the risk of a critical ramp/event that is about to occur, while some data
630 assimilation algorithms can dismiss outliers. The increased frequency of assimilation can address this
631 challenge. The frequency of assimilation is important for ramp prediction, while the challenge comes
632 from the model size and assimilation method chosen for the task, however simplified models with
633 higher frequencies can be adapted for the applications discussed here.

634 The work on data assimilation spans many disciplines and several decades in which many
635 different methods have been developed to adapt the state of the atmosphere in numerical weather
636 prediction models to large sets of measurements [97,98]. The initial development of data assimilation
637 has started as an objective analysis [e.g., 99,100], which is also referred to as successive correction
638 methods.

639 This work was followed by optimum interpolation (OI) [e.g. 97,101]. Optimal Interpolation (OI)
640 methods have lead to development of variational methods in data assimilation, where constraints
641 were introduced in variational data assimilation methods. These methods are namely 1DVAR,
642 2DVAR, 3DVAR [e.g. 102,103] and 4DVAR [104,105, e.g.,] where D stands for Dimension. Variational
643 approaches can be also formulated in the context of a Bayesian problem.

644 In parallel Kalman filter based approaches were developed [e.g. 106,107]. The Kalman filter is a
645 sequential data assimilation technique and was introduced as an observer feedback control system.
646 The main difference between 4DVar and Kalman filters are the way that they address the mode

and mean when the distributions are non-normal. There are several existing methods used in state estimation and/or data assimilation . Most of those methods build on the filtering theory introduced by Kalman and Bucy [108]. For the state estimation of linear Gaussian systems the original form of the Kalman filter has been widely applied. However, as it is linear it is not preferred for non-Gaussian and nonlinear systems [109,110]. Therefore techniques such as extended Kalman filter (EKF), ensemble Kalman filter (EnKF), unscented Kalman filter (UKF) and particle filter (PF) algorithms were developed [109,110] and applied to a wide range of use cases from low to high dimensional systems. EnKF method employs the linearization of the non-linearities with a Jacobian matrix, and also employs Monte-Carlo methods to estimate the background covariance errors to introduce nonlinearities to Kalman filter [e.g. 106,111–113]

Möhrlen et al. [36] found that some of the Kalman filter limitations in a meteorological context are however not a limitation in the wind power context, because the area of observational distribution is rather small, even if the area spans over an entire country. In atmospheric data assimilation the measurement data used is spread widely in space (globally), but is mostly sparse in time. In a wind power context, observations are concentrated in small areas with high time resolution. A classical KF approach would not make sense as models would have to generate forecasts in a small area, which is undesired, or it would require unrealistically many computing resources and observational input of meteorological variables [36]. The physical based ensemble prediction methods, especially the multi-scheme approach, has been found as the most efficient method due to its ability to generate spread that has a physical/meteorological meaning in any time step with a much smaller ensemble size [114].

One non-exclusive approach that can address the above approximations on nonlinearities and Gaussianity is particle filter (PF) however it brings the computational cost with it [115]. The computational cost is also related to ensemble size however this can be addressed adaptively with careful selection of ensembles introduced by Uzunoğlu [116]. The computational complexity in the above summarized methods can be addressed in the subspace of ensembles that was one of the focuses of the Maximum Likelihood Ensemble Filter (MLEF) that employs ensembles in the pre-conditioner. The computational time is reduced by optimizing a nonlinear cost function in low dimensional sampling space for Hessian information through maximum likelihood practice which also addresses the stochasticity and the discontinuity. This method has been applied to many disciplines such as power systems as well as to the wind energy industry [27,117]. In the workshop, the successful application of this method to second scales were presented.

5.4. Extreme event forecasting models

Extreme events in a meteorological sense are events that deviate from the mean and exceed beyond specific threshold limits. In the power system, extreme events can occur under meteorological average conditions as well and not be considered extreme, when meteorological threshold values, such as wind speed, are exceeded. The differences are mainly due to constraints in the transmission lines and the supply and demand relationship. Only in areas where wind turbines shut down due to high wind speeds- so called high-speed shutdowns, can such wind speeds challenge both life and the ability to safely control the grid.

The way to deal with extreme events in both meteorology and the power industry is by applying uncertainty forecasts that provide an objective measure of the possible extreme. Deterministic forecasts cannot serve such situations, as they are tuned for best average conditions, i.e. in the setup, statistical training and model output statistics, outliers and extremes are filtered out. While statistical approaches can be used in many life science applications, in power system applications it is crucial to employ an approach that provides a valid uncertainty of the forecast inclusive of extremes in every hour of the forecast. Such extreme forecasts must be established based on probabilities computed from a probabilistic prediction system that can take the spatial and temporal scales into consideration in order

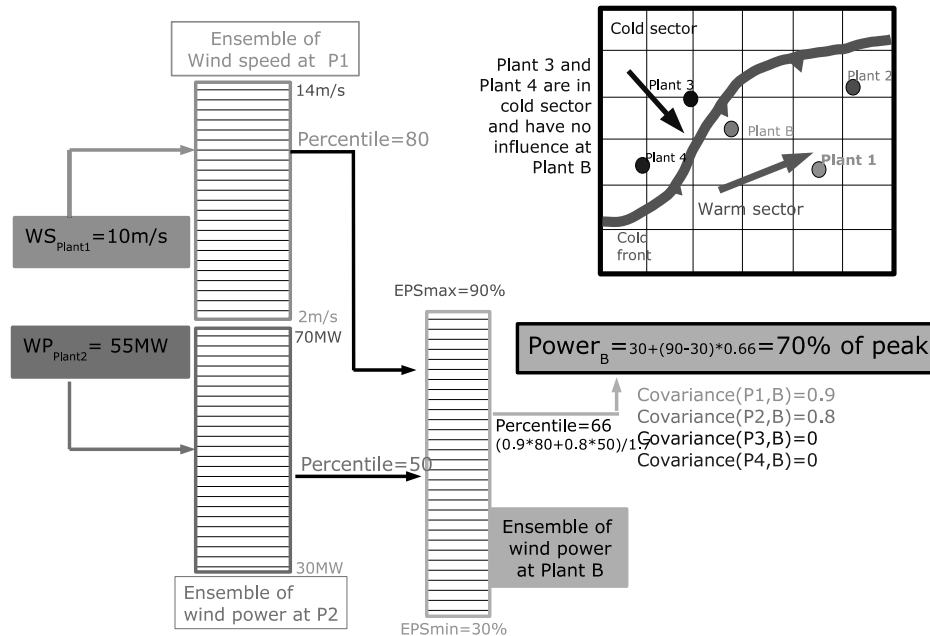


Figure 7. Functionality of the inverted Ensemble Kalman Filter when using different kind of measurements. P stands for Plant.

695 to capture the temporal evolution and spatial scale of e.g. low pressure systems that contain wind
696 speeds leading to large scale shut-down of wind farms.

697 This can for example be provided by a physical approach based on a NWP ensemble that ideally
698 contains all extreme values inherent in the approach without the requirement of statistical training such
699 as the multi-scheme method. Alternative solutions may exist from statistical approaches by employing
700 an extreme event analysis to a statistical ensemble [see e.g., 93]. However, statistical approaches
701 are always limited to past climatology and require large amounts of data. The requirement for such
702 forecasts is that they must be able to provide probabilities of extreme events, where each forecast or
703 "forecast member" provides a valid and consistent scenario of the event. The probabilities need to be
704 suitable solutions for a decision process. They can be computed for very critical and less critical events,
705 depending on the end-users' requirements.

706 In meteorology the use of sophisticated observational instrumentation for data assimilation
707 problems is an ongoing transformation throughout the last decades. As new technologies become
708 available that in some way are able to reflect some part of the atmospheric system, where the model
709 systems require parameterizations, such instrumentation is usually tested in research campaigns
710 and then deployed at specific locations [see e.g., 114,118–121]. Transferring this knowledge to
711 the assimilation of wind power observations that are irreversible in their nature is more complex.
712 Nevertheless, a unified methodology that is able to decide on the value of an observational signal and
713 its impact on the total system is required to solve this task.

714 In section 5.1.2 we learned that radar measurements can be used for forecasting, but require
715 transformation algorithms to be useful for the forward propagation of the data signals. The Kalman
716 Filter techniques are practical approaches that have inherent capabilities to transform such data signals
717 and use them in convective-scale data assimilation tasks (see e.g. [120,121]).

718 With ensemble Kalman filter techniques, the input ensemble data can also be used to deal with
719 the uncertainty of different types of measurements, also in the transformation phase of more advanced
720 data signal technologies if the signals are in relation with the target parameter [36]. The example

in Figure 7 shows the functionality of an inverted Kalman Filter approach for the assimilation of point measurements in (wind and solar) power space with a multi-scheme ensemble approach described in [36]. In this schematic, power signals from wind and/or solar generating units and other related meteorological observation are assimilated with the help of a so-called multi-scheme ensemble, a physical based ensemble approach [36]. The ensemble contains 75 members with 13 different parameterisation schemes, 10 from the physical part of the model and 3 dynamical parameterization schemes. Details of this system can be found in [38,122]. By applying physically possible outcomes from a 3-dimensional simulation of the atmosphere and transforming this into a vector in direct relation to the observation, a physically consistent data assimilation is possible. This approach is a major improvement and enhancement in energy meteorology as it opens the door to resolutions in time and space with minimal computational requirements for short-term or minute-scale forecasting, as the computational expensive work resides in the 6-hourly forecasting cycle of the ensemble. The assimilation of local measurements can be done on minute basis [36].

5.5. Overview of methods for minute-scale forecasting

Table 4 provides an overview and summary of the different minute-scale prediction methods, their forecasting horizons as well as advantages and limitations to the adoption of the methods. It also lists next steps that are suggested as a way to overcome the limitations.

During the discussions at the workshop and also whilst writing this paper, it became clear that as of now we are not in a position to recommend a minute-scale forecasts method that performs well in all conditions and for all use cases. Depending on the data input and the method, there are certain advantages and limitations that are inherent to the respective forecast types and methods. Remote sensing-based models for example work with preview data of the wind field several kilometers upstream of a wind turbine, but rely on the data availability of the remote sensing device which strongly depends on atmospheric conditions. Time series models are flexible in terms of input data, have a proven track record in power forecasting and have been used to a great extent across multiple disciplines. However, they rely on historical data and are therefore not likely to perform well for events outside of normal conditions. Data assimilation models have a wide range of applicability and can incorporate different types of measurements, but there is a lack of experience in the wind power industry.

What we propose as next steps for all methods are further investigations of the methods for different use cases, and also a cross-disciplinary exchange of different method experts. Remote sensing and NWP experts for example have to work together to see what the benefit in assimilating scanning-lidar data into a physical model is. Neural-network experts could implement real-time preview data from radar devices and investigate the possibility to forecast wind ramps when not only relying on historical data. The solution to minute-scale forecasting will possibly lie in the diversity of available input data and a forecasting method, that is tailored to the end user's needs.

Table 4. Overview of methods for minute-scale forecasting.

Type	Method	Input Data	Forecast Horizon	Advantages	Limitations	Next steps	Ref.
Remote sensing based models	Scanning lidar-based propagation models	Lidar data	1s–30 min	<ul style="list-style-type: none"> - Comprehensive knowledge of wind field several kilometres upstream - Scanning of vertical wind profiles for e.g. detection of low level jets - Compact size → flexible measurement campaigns, cost-competitive to met masts 	<ul style="list-style-type: none"> - Fluctuating measurement range and forecast horizon due to environmental conditions - Ideal measurement setup for forecasting not clear, no standard available - Need for post processing is challenging in a real-time environment 	<ul style="list-style-type: none"> - Need for a reliable fallback method if no data available - Investigation of different lidar cases to find best campaign setup → standards definition. - Regular service and calibration → decreases risk of faulty signal processing but increases costs. 	[14,42, 45,46, 49,50, 57]
	Radar-based density models	Doppler radar data	1min–<1h	<ul style="list-style-type: none"> - Extended maximum measurement range (up to 35 km) - Reconstructed wind fields with high temporal (1-min) and spatial (50 m) resolution - Volumetric measurements allow to resolve information over the whole rotor area 	<ul style="list-style-type: none"> - Data availability highly depends on the meteorological conditions - Large beam spread at large ranges → increased uncertainty - Large dimensions of the radar → complex installation 	<ul style="list-style-type: none"> - Explore deeply and define the conditions and locations for optimal measurements - Investigate added value of installing a radar system for ramp event prediction in a wind farm cluster 	[64,65]
	Radar-based power fluctuation forecast	C and X-band weather radar data	10min–2h	<ul style="list-style-type: none"> - Precipitation data highly correlates with strong fluctuations - Extended maximum measurement range → 60–240 km - Spatial resolution: 0.5–2 km / Temporal resolution: 1–15 minutes 	<ul style="list-style-type: none"> - Clutter due to: wind turbine interference, meteorological targets - Measurement uncertainty increases with precipitation intensity - Underestimation of precipitation reflectivity during convective events 	<ul style="list-style-type: none"> - Further development of pattern recognition techniques is required - Investigation on new wind turbine clutter detection and mitigation techniques - Improve cooperation between weather radars and wind energy communities 	[66,67]
Time series models	AR AR(I)MA	SCADA, met-mast data, remote sensing	30s–24h	<ul style="list-style-type: none"> - Easy to implement and demonstrates higher skill than persistence for most lead times - Proven track record in power forecasting and a large volume of reference work across quantitative disciplines on how to design, build, and validate models 	<ul style="list-style-type: none"> - Relies on historical data, therefore not likely to perform well for events outside of normal conditions - Data quality concerns for e.g. sensor faults 	<ul style="list-style-type: none"> - Collect, store, and label high-frequency data for building and testing statistical models at the 1s–10min horizons - Utilize statistical model benchmarks in all minute-scale forecasting trials for comparison 	[72–74, 83]
	Neural networks	Same as above	15s–24h	<ul style="list-style-type: none"> - Ability to learn complex non-linear relationships - Flexible model construction in terms of inputs/outputs compared to ARIMA methods 	<ul style="list-style-type: none"> - Computationally demanding, large datasets required for training and validation - Requires significant background knowledge to understand and implement added complexity not always an improvement 	<ul style="list-style-type: none"> - Continue monitoring developments as the field is rapidly evolving - Leverage this power and flexibility to extract value from high dimensional data (e.g. from remote sensing instruments) 	[75,76, 80]
Data assimilation models	VAR models	lidar, radar, sodar, cup / sonic anemometers	look ahead time 3h–12h for analysis, forecast 1min–12h	<ul style="list-style-type: none"> - Methods have a wide range of applicability and can incorporate different types of measurements - Extreme event analysis benefits from a diversity of observations - Expensive ensemble computations not required on minute scale, but e.g. 6h-schedule – inverted EnKF: first weather dependent short-term algorithm for wind power apps 	<ul style="list-style-type: none"> - Lack of use cases in power industry to prove the value of such information - Lack of standards and transparency of data exchange in power markets 	<ul style="list-style-type: none"> - Setting up measurement campaigns with open data access for research and development - Increased collaborative research between meteorology and wind power forecasting community 	[27,36, 70,71, 114]

757 6. Challenges for the implementation of minute-scale forecasting in large energy systems

758 There are several use cases for predictions shorter than 1 to 2 hours. In Australia, the system
759 runs on a 5-min schedule [123] and requires renewable energy and load forecasts on those time scales.
760 In Germany, renewable energy plants can be pre-qualified to participate in the reserve market, and
761 need to predict their possible power with less than 5% error in the pilot phase and less than 3.3% in
762 the implementation phase. This is calculated in one-minute intervals. In Denmark, with hourly wind
763 penetrations of over 140%, the grid is run proactively in hourly steps, predicting the imbalance and
764 reacting accordingly on the basis of spatio-temporal forecasts [124]. So the use cases for minute scale
765 forecasts are present, and the best forecasts require upstream information in real time.

766 In a large energy system with moderate penetration from wind sources, a system operator can
767 choose to outsource balancing of wind. This is the approach chosen widely in central Europe. A major
768 reason behind the liberalized strategy in Europe is a wish to make the market more competitive which
769 has happened faster than anybody expected in both Denmark (2009) and Germany (2012) [125] with
770 the result of lower spot market prices in the NordPool market and the German-Austrian component of
771 EPEX.

772 The difference between a TSO and a power trader's prioritized optimization lies in the target
773 horizon. The trader is looking up to several weeks ahead, while the TSO's optimization horizon
774 is over the entire year. In particular once the power trading is privatized and handled by private
775 balance responsible parties, then the TSO lacks information about the generation and must rely on the
776 information from the trading companies. In Germany, the TSOs have today little control of renewable
777 energy generation and rely on out-sourced solutions for critical system information to a large degree
778 which has not been considered acceptable for many years from a system security perspective.

779 Although Germany has the highest capacity of wind and solar generation in Europe, it is apparent
780 that the system lacks information for optimization. This is seen in frequent downregulation of wind
781 farms during day-time and recovery during the middle of the night, often many hours after the wind
782 has dropped again. This process has become highly inefficient in recent years, because there are no
783 requirements for wind farms to provide real-time data to the system operator.

784 The German experience shows that wind energy loses efficiency and value unless there are
785 obligations for wind farms to provide data required by various forecasting and system operation
786 processes.

787 Based on this experience, it is crucial to define standards regarding the setup and maintenance
788 of instrumentation, collection and provision of data, as well as required quality of data. Beside the
789 standards, in transparent markets the grid codes should also contain a clear definition about the rights
790 on the use and the obligation to provide the data. Without such regulations, the required quality is
791 hard to achieve in order to improve forecasts. Corrupt and wrongly calibrated instrumentation can do
792 more damage to a forecast than not having data. This is one of the greatest challenges at present and
793 the reason for slow progress on minute-scale forecasting. Especially in large systems such as Germany
794 with many thousands of individual wind turbines and small wind farms, this is a difficult challenge to
795 overcome. Nevertheless, the need to make appropriate changes to the grid codes is the same for all
796 markets.

797 7. Conclusions

798 Minute-scale forecasting of wind power is a discipline that is becoming crucial to accomplish in
799 globally transitioning power systems with increasing amounts of variable generating power sources
800 from renewables. The participants of the collaborative IEA Wind Task 32 and 36 workshop have
801 established a framework for forecasting at the minute scale and have discussed new techniques that
802 will push the limits of state-of-the-art forecasting methods.

803 Three applications were identified that can benefit from minute-scale forecasting and their
804 respective forecasting horizons. Wind turbine and wind farm controllers need wind speed forecasts
805 with the shortest horizon to optimize the turbine and farm operation. The task of balancing the power

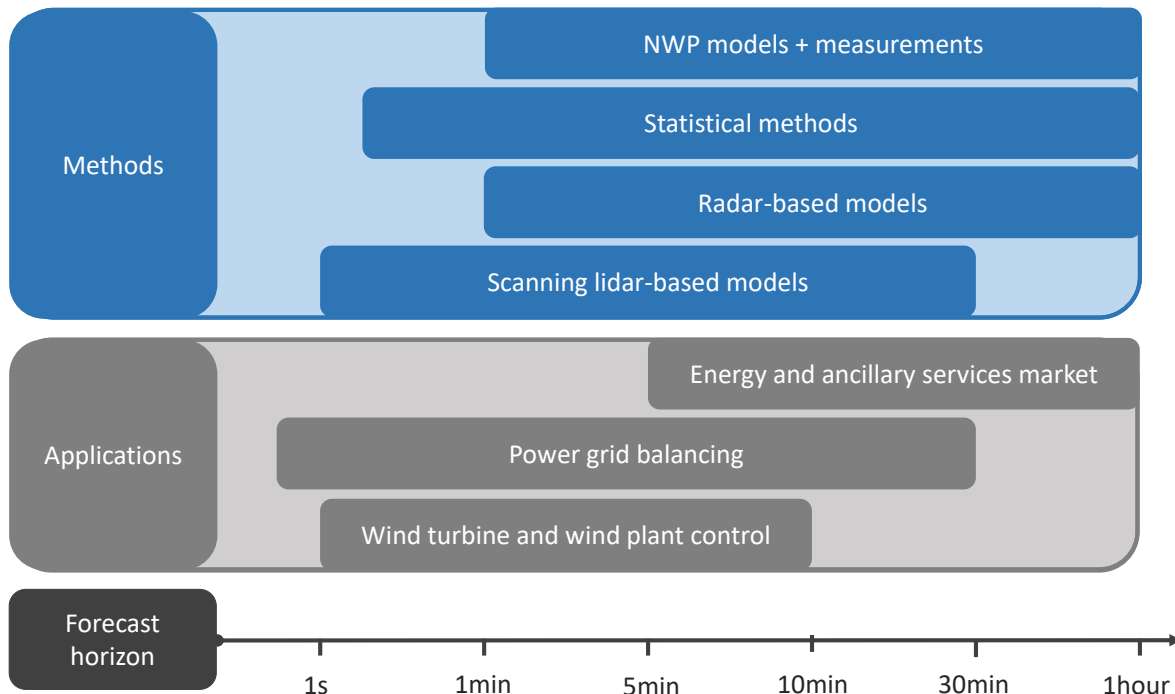


Figure 8. Overview of forecast horizons of different wind energy applications and forecast methods in the second and minute scale.

grid, and finally optimizing energy markets which rely heavily on precise wind power forecasts on a slightly longer time scale as well.

To carry out forecasts that range from 1 second to 60 minutes, forecasters have the choice between different methods (Figure 8). In our discussions at the workshop and this review paper we differentiate between using preview data from remote sensing devices, time series models that deduce patterns from observational data to predict future values and finally methods that are based on data assimilation into physical models. These assimilated data can originate both from remote sensing devices or other existing observational data sources i.e. meteorological masts and wind turbine data.

By investigating more deeply the respective methods it became clear that they all have advantages, but also limitations that need to be overcome in order to achieve reliable forecasts for commercial use. The following list provides an overview of focus areas for the near future to advance further with minute-scale forecasting:

- **Research requirements.** At this point, many methods are still under development. There are several open questions to solve and the optimal forecasting techniques for the different applications have not been concluded. It is also not sufficiently demonstrated that all methods add value. More research and especially more measurement campaigns using different types of instrumentation (lidars, radars, sodars and in situ measurements such as cup and sonic anemometers etc.) to compare their benefits and disadvantages as individual inputs but also as combinations of inputs is required. Both measurement experts and weather modelers need to collaborate closely to find solutions.
- **Data requirements.** All forecasting methods rely on data. This might sound obvious, but what is needed is high resolution, high quality data delivered in real-time to forecast systems. Wind turbine or wind farm operators often only log 10-minute averages of their operational data. However, to train and validate models, high frequency data is necessary.
- **Requirement for standards.** End users have more confidence in data when the collection and use of the data is supported by Recommended Practices and standards. Community-driven

832 recommended practices are available for some applications of wind lidar, but not in the context
833 of forecasting.

- 834 • **Expert training.** As with any emerging technology, there are a limited number of experts that
835 know how to carry out a remote sensing measurement campaign, feed data into neural networks
836 or are capable of assimilating data into a NWP model. This forms a barrier to the widespread
837 commercialization of minute-scale forecasting. IEA Wind Tasks provide an ideal platform for
838 the international exchange and dissemination of knowledge order to establish more widespread
839 training in the above mentioned areas.

840 **Supplementary Materials:** IEA Wind Task 32 is operated by the Chair of Wind Energy at the Institute of Aircraft
841 Design at the Faculty of Aerospace Engineering at the University of Stuttgart. More details about IEA Wind
842 Task 32, including minutes from the workshops and other documents, can be found at www.ieawindtask32.org. IEA Wind Task 36 Forecasting is operated by Gregor Giebel of DTU Wind Energy at Risø, Denmark.
843 See www.ieawindforecasting.dk for more information. General information about IEA Wind can be found at
844 www.ieawind.org. IEA Wind TCP functions within a framework created by the International Energy Agency.
845 Views, findings, and publications of the IEA Wind TCP do not necessarily represent the views or policies of the
846 IEA Secretariat or of all its individual member countries. IEA Wind TCP is part of IEA's Technology Collaboration
847 Programme (TCP).

848 **Author Contributions:** Ines Würth was a co-organizer of the workshop, led the paper and wrote the abstract,
849 introduction, Section 5.1.1, conclusion, some section introductions, and edited all sections. Laura Valldecabres
850 Sanmartin was a co-organizer of the workshop, was a co-editor of this paper, led Section 2, 3.3 and 5.1.2 and
851 contributed to Section 5.1.1, and 5.1. Elliot Simon was a co-organizer of the workshop, led Section 5.2, and
852 contributed in Sections: 2, 5.1.1, 5.1, and 5.5. David Schlipf led Section 3.1. Bahri Uzunoğlu led Section 3.2 and
853 wrote Section 5.3 and 5.4 together with Corinna Mörlen who also led Section 4 and 5.1.4 and contributed to Section
854 5.1, 5.2, 3.3 and 6. Gregor Giebel contributed to Section 4. Ciaran Gilbert contributed to Section 5.2. Anton Kaifel
855 and all other co-authors participated in the paper review and revision process.

856 **Funding:** This publication was supported by the Open Access Publishing Fund of the University of Stuttgart and
857 has received funding from the European Union's Horizon 2020 research and innovation programme under the
858 Marie Skłodowska-Curie Grant No. 642108.

859 **Acknowledgments:** We would like to thank DTU Wind Energy (Risø campus) for graciously hosting the workshop,
860 and all of the workshop participants who contributed their ideas and knowledge.

861 **Conflicts of Interest:** The authors declare no conflict of interest.

863 References

- 864 1. Giebel, G.; Brownsword, R.; Kariniotakis, G.; Denhard, M.; Draxl, C. The State-Of-The-Art in Short-Term
865 Prediction of Wind Power. Technical report, Technical University of Denmark (DTU), Roskilde, Denmark,
866 2011. doi:10.11581/DTU:00000017.
- 867 2. Fraile, D.; Mbistrova, A. Wind in power 2017: Annual combined onshore and offshore wind energy
868 statistics. Technical report, WindEurope, 2018.
- 869 3. Fraile, D.; Komusanac, I. Wind energy in Europe: Outlook to 2022. Technical report, WindEurope, 2018.
- 870 4. Larsén, X.; Larsen, S.; Lundtang Petersen, E. Full-Scale Spectrum of Boundary-Layer Winds. *Boundary-Layer
871 Meteorology* **2016**, *159*, 349–371. doi:10.1007/s10546-016-0129-x.
- 872 5. Apt, J. The spectrum of power from wind turbines. *Journal of Power Sources* **2007**, *169*, 369–374.
873 doi:10.1016/j.jpowsour.2007.02.077.
- 874 6. Vincent, C.L.; Trombe, P.J. 8 - Forecasting intrahourly variability of wind generation. In *Renewable Energy
875 Forecasting*; Kariniotakis, G., Ed.; Woodhead Publishing Series in Energy, Woodhead Publishing, 2017; pp.
876 219 – 233. doi:<https://doi.org/10.1016/B978-0-08-100504-0-00008-1>.
- 877 7. Sørensen, P.; Cutululis, N.A.; Vigueras-Rodríguez, A.; Madsen, H.; Pinson, P.; Jensen, L.E.; Hjerrild, J.;
878 Donovan, M. Modelling of power fluctuations from large offshore wind farms. *Wind Energy* **2008**, *11*, 29–43.
879 doi:10.1002/we.246.
- 880 8. Akhmatov, V.; Abildgaard, H.; Pedersen, J.; Eriksen, P. Integration of Offshore Wind Power into the
881 Western Danish Power System. *Proc. Copenhagen Offshore Wind 2005* **2005**.
- 882 9. van Kooten, G.C. Wind power: the economic impact of intermittency. *Letters in Spatial and Resource Sciences*
883 **2010**, *3*, 1–17. doi:10.1007/s12076-009-0031-y.

- 884 10. Ela, E.; Kirby, B. ERCOT Event on February 26, 2008: Lessons Learned. Technical report, National
885 Renewable Energy Laboratory, 2008. doi:10.2172/1218412.
- 886 11. Gallego-Castillo, C.; Cuerva-Tejero, A.; Lopez-Garcia, O. A review on the recent history of
887 wind power ramp forecasting. *Renewable and Sustainable Energy Reviews* **2015**, *52*, 1148 – 1157.
888 doi:10.1016/j.rser.2015.07.154.
- 889 12. Würth, I.; Ellinghaus, S.; Wigger, M.; Niemeier, M.J.; Clifton, A.; Cheng, P.W. Forecasting wind
890 ramps: can long-range lidar increase accuracy? *Journal of Physics: Conference Series* **2018**, *1102*, 012013.
891 doi:10.1088/1742-6596/1102/1/012013.
- 892 13. Dunne, F.; Pao, L.Y.; Schlipf, D.; Scholbrock, A.K. Importance of lidar measurement timing
893 accuracy for wind turbine control. *2014 American Control Conference*, 2014, pp. 3716–3721.
894 doi:10.1109/ACC.2014.6859337.
- 895 14. Schlipf, D. Lidar-Assisted Control Concepts for Wind Turbines. PhD thesis, University of Stuttgart, 2015.
896 doi:10.18419/opus-8796.
- 897 15. Gros, S. An economic NMPC formulation for wind turbine control. Proceedings of the Conference on
898 Decision and Control; , 2013.
- 899 16. Schlipf, D.; Schlipf, D.J.; Kühn, M. Nonlinear model predictive control of wind turbines using LIDAR.
900 *Wind Energy* **2013**, *16*, 1107–1129. doi:10.1002/we.1533.
- 901 17. Hau, E. *Wind Turbines: Fundamentals, Technologies, Application, Economics*; Springer, 2006.
- 902 18. Kragh, K.A.; Hansen, M.H.; Mikkelsen, T. Improving Yaw Alignment Using Spinner Based LIDAR.
903 Proceedings of the 49th AIAA Aerospace Sciences Meeting Including the New Horizons Forum and
904 Aerospace Exposition; , 2011.
- 905 19. Schlipf, D.; Kapp, S.; Anger, J.; Bischoff, O.; Hofsfäss, M.; Rettenmeier, A.; Smolka, U.; Kühn, M. Prospects
906 of Optimization of Energy Production by LiDAR Assisted Control of Wind Turbines. Proceedings of the
907 European Wind Energy Association annual event; , 2011.
- 908 20. Bossanyi, E. Combining induction control and wake steering for wind farm energy and fatigue loads
909 optimisation. *J. Phys.: Conf. Ser.* **2018**, *1037*. doi:10.1088/1742-6596/1037/3/032011.
- 910 21. Ela, E.; Gevorgian, V.; Fleming, P.; Zhang, Y.; Singh, M.; Muljadi, E.; Scholbrook, A.; Aho, J.; Buckspan,
911 A.; Pao, L.; Singhvi, V.; Tuohy, A.; Pourbeik, P.; Brooks, D.; Bhatt, N. Active power controls from wind
912 power: Bridging the gaps. Technical report, National Renewable Energy Laboratory, Golden, Colorado,
913 USA, 2014.
- 914 22. Gebraad, P.M.O. Data-driven wind plant control. PhD thesis, Delft University of Technology, 2014.
915 doi:10.4233/uuid:5c37b2d7-c2da-4457-bff9-f6fd27fe8767.
- 916 23. Momoh, J.A. *Smart grid: fundamentals of design and analysis*; Vol. 63, John Wiley & Sons, 2012.
- 917 24. Menin, M.; Uzunoglu, B. Parametric Sensitivity Study for Wind Power Trading through Stochastic Reserve
918 and Energy Market Optimization. *2015 Seventh Annual IEEE Green Technologies Conference*, 2015, pp.
919 82–87. doi:10.1109/GREENTECH.2015.37.
- 920 25. Uzunoglu, B.; Bayazit, D. A generic resampling particle filter joint parameter estimation for electricity
921 prices with jump diffusion. *2013 10th International Conference on the European Energy Market (EEM)*,
922 2013, pp. 1–7. doi:10.1109/EEM.2013.6607409.
- 923 26. Uzunoglu, B.; AkifÜlker, M.; Bayazit, D. Particle filter joint state and parameter estimation of dynamic
924 power systems. *2016 57th International Scientific Conference on Power and Electrical Engineering of Riga
925 Technical University (RTUCON)*, 2016, pp. 1–7. doi:10.1109/RTUCON.2016.7763152.
- 926 27. Uzunoğlu, B.; Ülker, M.A. Maximum Likelihood Ensemble Filter State Estimation for Power Systems.
927 *IEEE Transactions on Instrumentation and Measurement* **2018**, *67*, 2097–2106. doi:10.1109/TIM.2018.2814066.
- 928 28. Ülker, M.A.; Uzunoğlu, B. Simplex optimization for particle filter joint state and parameter estimation of
929 dynamic power systems. *IEEE EUROCON 2017 -17th International Conference on Smart Technologies*,
930 2017, pp. 399–404. doi:10.1109/EUROCON.2017.8011142.
- 931 29. Eriksson, R.; Modig, N.; Elkington, K. Synthetic inertia versus fast frequency response: a definition. *IET
932 Renewable Power Generation* **2018**, *12*, 507–514. doi:10.1049/iet-rpg.2017.0370.
- 933 30. Díaz-González, F.; Haub, M.; Sumper, A.; Gomis-Bellmuntac, O. Participation of wind power plants
934 in system frequency control: Review of grid code requirements and control methods. *Renewable and
935 Sustainable Energy Reviews* **2014**, *43*, 551–564. doi:10.1016/j.rser.2014.03.040.

- 936 31. Mazzi, N.; Pinson, P. 10 - Wind power in electricity markets and the value of forecasting. In *Renewable
937 Energy Forecasting*; Kariniotakis, G., Ed.; Woodhead Publishing Series in Energy, Woodhead Publishing,
938 2017; pp. 259 – 278. doi:<https://doi.org/10.1016/B978-0-08-100504-0.00010-X>.
- 939 32. EPEX Spot SE. *Intraday Continous: Intraday Lead Times*, (accessed December 10, 2018).
- 940 33. NordPool. *Intraday Trading*, (accessed December 10, 2018).
- 941 34. Energy Exchange Istanbul (EXIST). *Intra-day Market*, (accessed December 10, 2018). <https://www.epias.com.tr/en/intra-day-market/phases>.
- 942 35. BSP South Pool. *Intraday Continous Market*, (accessed December 10, 2018). <https://www.bsp-southpool.com/intraday-continuous-market.html>.
- 943 36. Möhren, C., J.J. A new algorithm for Upscaling and Short-term forecasting of wind power using Ensemble
944 forecasts; Energynautics GmbH: Bremen, Germany, 2009.
- 945 37. 50Hertz.; Ampriion.; Tennet.; TransnetBW. Leitfaden zur Präqualifikation von Windenergieanlagen zur
946 Erbringung von Minutenreserveleistung im Rahmen einer Pilotphase / Guidelines for Prequalification of
947 Wind Turbines to provide Minute Reserves during a Pilot Phase. Technical report, German Transmission
948 System Operators: Germany, German Transmission System Operators: Germany, 2016.
- 949 38. Pahlow, M.; Möhrlen, C.; Jørgensen, J., Application of cost functions for large-scale integration of wind
950 power using a multi-scheme ensemble prediction technique; Optimization Advances in Electric Power
951 Systems, NOVA Publisher NY, 2008.
- 952 39. IEC. Wind energy generation systems - Part 12-1: Power performance measurements of electricity
953 producing wind turbines. Standard, International Electrotechnical Commission, Geneva, CH, 2017.
- 954 40. Clifton, A.; Clive, P.; Gottschall, J.; Schlipf, D.; Simley, E.; Simmons, L.; Stein, D.; Trabucchi, D.; Vasiljevic,
955 N.; Würth, I. IEA Wind Task 32: Wind Lidar - Identifying and mitigating barriers to the adoption of wind
956 lidar. *Remote Sensing* **2018**, *10*, 413–433. doi:10.3390/rs10030406.
- 957 41. Emeis, S.; Harris, M.; Banta, R.M. Boundary-layer anemometry by optical remote sensing for wind energy
958 applications. *Meteorologische Zeitschrift* **2007**, *16*, 337–347. doi:10.1127/0941-2948/2007/0225.
- 959 42. Simley, E.; Pao, L.Y.; Frehlich, R.; Jonkman, B.; Kelley, N. Analysis of light detection and ranging wind
960 speed measurements for wind turbine control. *Wind Energy* **2014**, *17*, 413–433. doi:10.1002/we.1584.
- 961 43. Clifton, A.; Boquet, M.; Burin Des Roziers, E.; Westerhellweg, A.; Hofsass, M.; Klaas, T.; Vogstad, K.; Clive,
962 P.; Harris, M.; Wylie, S.; Osler, E.; Banta, B.; Choukulkar, A.; Lundquist, J.; Aitken, M. Remote Sensing
963 of Complex Flows by Doppler Wind Lidar: Issues and Preliminary Recommendations. Technical Report
964 TP-5000-64634, National Renewable Energy Laboratory, 2015.
- 965 44. Vasiljević, N.; L. M. Palma, J.M.; Angelou, N.; Carlos Matos, J.; Menke, R.; Lea, G.; Mann, J.; Courtney, M.;
966 Frölen Ribeiro, L.; M. G. C. Gomes, V.M. Perdigão 2015: methodology for atmospheric multi-Doppler lidar
967 experiments. *Atmospheric Measurement Techniques* **2017**, *10*, 3463–3483. doi:10.5194/amt-10-3463-2017.
- 968 45. Courtney, M.; Simon, E. *Deploying scanning lidars at coastal sites*; DTU Wind Energy: Denmark, 2016.
- 969 46. Valdecabres, L.; Peña, A.; Courtney, M.; von Bremen, L.; Kühn, M. Very short-term forecast of near-coastal
970 flow using scanning lidars. *Wind Energy Science* **2018**, *3*, 313–327. doi:10.5194/wes-3-313-2018.
- 971 47. Simon, E.; Courtney, M.; Vasiljevic, N. Minute-Scale Wind Speed Forecasting Using Scanning Lidar Inflow
972 Measurements. *Wind Energy Science Discussions* **2018**. doi:10.5194/wes-2018-71.
- 973 48. Kokhanovsky, A. *Aerosol Optics: Light Absorption and Scattering by Particles in the Atmosphere*; Springer-Verlag
974 Berlin Heidelberg, 2008.
- 975 49. Würth, I.; Brenner, A.; Wigger, M.; Cheng, P.W. How far do we see? Analysis of the measurement range of
976 long-range lidar data for wind power forecasting. German Wind Energy Conference DEWEK, 2017.
- 977 50. Performance Verification of Galion. Technical Report Report 13001, Deutsche Windguard, 2013.
- 978 51. Bradley, S. Wind speed errors for LIDARs and SODARs in complex terrain. *IOP Conference Series: Earth
979 and Environmental Science* **2008**, *1*, 012061.
- 980 52. Bradley, S.; Perrott, Y.; Behrens, P.; Oldroyd, A. Corrections for wind-speed errors from Sodar and Lidar in
981 complex terrain. *Boundary-Layer Meteorology* **2012**, *143*, 37–48. doi:10.1007/s10546-012-9702-0.
- 982 53. Bradley, S.; von Hünerbein, S.; Mikkelsen, T. A bistatic Sodar for precision wind profiling in complex
983 terrain. *Journal of Atmospheric and Oceanic Technology* **2012**, *29*, 1052–1061. doi:10.1175/JTECH-D-11-00035.1.
- 984 54. Emeis, S.; Harris, M.; Banta, R.M. Boundary-layer anemometry by optical remote sensing for wind energy
985 applications. *Meteorologische Zeitschrift* **2007**, *16*, 337–347. doi:10.1127/0941-2948/2007/0225.

- 988 55. Kindler, D.; Oldroyd, A.; MacAskill, A.; Finch, D. An eight month test campaign of the Qinetiq ZephIR
989 system: Preliminary results. *Meteorologische Zeitschrift* **2007**, *16*, 479–489. doi:10.1127/0941-2948/2007/0226.
- 990 56. Yang, Q.; Berg, L.; Pekour, M.; Fast, J.; Newsom, R. Evaluation of WRF-Predicted Near-Hub-Height Winds
991 and Ramp Events over a Pacific Northwest Site with Complex Terrain. *J. of Appl. Meteo. and Climatology*
992 **2013**, *52*, 1753–1763. doi:10.1175/JAMC-D-12-0267.1.
- 993 57. Clifton, A.; M.Boquet.; Burin, E.; Hofsäß, M.; Klaas, T.; Vogstad, K.; Clive, P.; Harris, M.; Wylie, S.; E.Osler.;
994 Banta, R.; Choukulkar, A.; Lundquist, J.; Aitken., M. Remote Sensing of Complex Flows by Doppler
995 Wind Lidar: Issues and Preliminary Recommendations. Technical report, National Renewable Energy
996 Laboratory, 15013 Denver West Parkway, Golden, CO 80401, 2015.
- 997 58. Vasiljević, N.; L. M. Palma, J.M.; Angelou, N.; Carlos Matos, J.; Menke, R.; Lea, G.; Mann, J.; Courtney, M.;
998 Frölen Ribeiro, L.; M. G. C. Gomes, V.M. Perdigão 2015: methodology for atmospheric multi-Doppler lidar
999 experiments. *Atmospheric Measurement Techniques* **2017**, *10*, 3463–3483. doi:10.5194/amt-10-3463-2017.
- 1000 59. Wulfmeyer, V.; Turner, D.D.; Baker, B.; Banta, R.; Behrendt, A.; Bonin, T.; Brewer, W.A.; Buban,
1001 M.; Choukulkar, A.; Dumas, E.; Hardesty, R.M.; Heus, T.; Ingwersen, J.; Lange, D.; Lee, T.R.;
1002 Metzendorf, S.; Muppa, S.K.; Meyers, T.; Newsom, R.; Osman, M.; Raasch, S.; Santanello, J.; Senff, C.;
1003 Späth, F.; Wagner, T.; Weckwerth, T. A New Research Approach for Observing and Characterizing
1004 Land–Atmosphere Feedback. *Bulletin of the American Meteorological Society* **2018**, *99*, 1639–1667,
1005 [<https://doi.org/10.1175/BAMS-D-17-0009.1>]. doi:10.1175/BAMS-D-17-0009.1.
- 1006 60. Hirth, B.D.; Schroeder, J.L.; Gunter, W.S.; Guynes, J.G. Measuring a Utility-Scale Turbine Wake Using
1007 the TTUKa Mobile Research Radars. *Journal of Atmospheric and Oceanic Technology* **2012**, *29*, 765–771.
1008 doi:10.1175/JTECH-D-12-00039.1.
- 1009 61. Hirth, B.D.; Schroeder, J.L.; Gunter, W.S.; Guynes, J.G. Coupling Doppler radar-derived wind maps
1010 with operational turbine data to document wind farm complex flows. *Wind Energy* **2015**, *18*, 529–540.
1011 doi:10.1002/we.1701.
- 1012 62. Nygaard, N.G.; Newcombe, A.C. Wake behind an offshore wind farm observed with dual-Doppler radars.
1013 *Journal of Physics: Conference Series* **2018**, *1037*, 072008. doi:10.1088/1742-6596/1037/7/072008.
- 1014 63. Marathe, N.; Swift, A.; Hirth, B.; Walker, R.; Schroeder, J. Characterizing power performance and wake of
1015 a wind turbine under yaw and blade pitch. *Wind Energy* **2016**, *19*, 963–978. doi:10.1002/we.1875.
- 1016 64. Hirth, B.D.; Schroeder, J.L.; Irons, Z.; Walter, K. Dual-Doppler measurements of a wind ramp event at an
1017 Oklahoma wind plant. *Wind Energy* **2016**, *19*, 953–962. doi:10.1002/we.1867.
- 1018 65. Valldcabres, L.; Nygaard, N.G.; Vera-Tudela, L.; von Bremen, L.; Kühn, M. On the Use of
1019 Dual-Doppler Radar Measurements for Very Short-Term Wind Power Forecasts. *Remote Sensing* **2018**, *10*.
1020 doi:10.3390/rs10111701.
- 1021 66. Trombe, P.J.; Pinson, P.; Vincent, C.; Bøvith, T.; Cutululis, N.A.; Draxl, C.; Giebel, G.; N.Hahmann, A.;
1022 E.Jensen, N.; Jensen, B.P.; Le, N.F.; Madsen, H.; Pedersen, L.B.; Sommer, A. Weather radars – the new eyes
1023 for offshore wind farms? *Wind Energy* **2014**, *17*, 1767–1787. doi:10.1002/we.1659.
- 1024 67. Trombe, P.; Pinson, P.; Madsen, H. Automatic Classification of Offshore Wind Regimes With Weather
1025 Radar Observations. *IEEE Journal of Selected Topics in Applied Earth Observations and Remote Sensing* **2014**,
1026 *7*, 116–125. doi:10.1109/JSTARS.2013.2252604.
- 1027 68. Freedman, J.M.; Manobianco, J.; Schroeder, J.; Ancell, B.; Brewster, K.; Basu, S.; Banunarayanan, V.;
1028 Hodge, B.M.; Flores, I. The Wind Forecast Improvement Project (WFIP): A Public/Private Partnership for
1029 Improving Short Term Wind Energy Forecasts and Quantifying the Benefits of Utility Operations. The
1030 Southern Study Area, Final Report **2014**. doi:10.2172/1129905.
- 1031 69. *Meteorological Assimilation Data Ingest System (MADIS)*, (accessed December 10, 2018).
- 1032 70. Wilczak, J.; Finley, C.; Freedman, J.; Cline, J.; Bianco, L.; Olson, J.; Djalalova, I.; Sheridan, L.; Ahlstrom,
1033 M.; Manobianco, J.; Zack, J.; Carley, J.R.; Benjamin, S.; Coulter, R.; Berg, L.K.; Mirocha, J.; Clawson, K.;
1034 Natenberg, E.; Marquis, M. The Wind Forecast Improvement Project (WFIP): A Public–Private Partnership
1035 Addressing Wind Energy Forecast Needs. *Bull. Amer. Meteor. Soc.* **2015**, *96*, 1699–1718.
- 1036 71. Nakafuji, D. Distributed Resource Energy Analysis & Management System (DREAMS) Development for
1037 Real-time Grid Operations. Technical Report DOE-EE0006331-FTR1, Hawaiian Electric Company to U.S.
1038 Department of Energy, 2016.

- 1039 72. Pinson, P. Very-short-term probabilistic forecasting of wind power with generalized logit–normal
1040 distributions. *Journal of the Royal Statistical Society: Series C (Applied Statistics)* **2012**, *61*, 555–576.
1041 doi:10.1111/j.1467-9876.2011.01026.x.
- 1042 73. Torres, J.; García, A.; Blas, M.D.; Francisco, A.D. Forecast of hourly average wind speed with ARMA models
1043 in Navarre (Spain). *Solar Energy* **2005**, *79*, 65 – 77. doi:<https://doi.org/10.1016/j.solener.2004.09.013>.
- 1044 74. Erdem, E.; Shi, J. ARMA based approaches for forecasting the tuple of wind speed and direction. *Applied
1045 Energy* **2011**, *88*, 1405 – 1414. doi:<https://doi.org/10.1016/j.apenergy.2010.10.031>.
- 1046 75. Li, G.; Shi, J. On comparing three artificial neural networks for wind speed forecasting. *Applied Energy*
1047 **2010**, *87*, 2313 – 2320. doi:<https://doi.org/10.1016/j.apenergy.2009.12.013>.
- 1048 76. Feng, C.; Cui, M.; Hodge, B.M.; Zhang, J. A data-driven multi-model methodology with
1049 deep feature selection for short-term wind forecasting. *Applied Energy* **2017**, *190*, 1245 – 1257.
1050 doi:<https://doi.org/10.1016/j.apenergy.2017.01.043>.
- 1051 77. Niu, T.; Wang, J.; Zhang, K.; Du, P. Multi-step-ahead wind speed forecasting based on optimal feature
1052 selection and a modified bat algorithm with the cognition strategy. *Renewable Energy* **2018**, *118*, 213–229.
1053 doi:10.1016/j.renene.2017.10.075.
- 1054 78. Pinson, P. Introducing distributed learning approaches in wind power forecasting. 2016
1055 International Conference on Probabilistic Methods Applied to Power Systems (PMAPS), 2016, pp. 1–6.
1056 doi:10.1109/PMAPS.2016.7764224.
- 1057 79. Hochreiter, S.; Schmidhuber, J. Long Short-Term Memory. *Neural Computation* **1997**, *9*, 1735–1780.
1058 doi:10.1162/neco.1997.9.8.1735.
- 1059 80. Wu, W.; Chen, K.; Qiao, Y.; Lu, Z. Probabilistic short-term wind power forecasting based on deep neural
1060 networks. 2016 International Conference on Probabilistic Methods Applied to Power Systems (PMAPS),
1061 2016, pp. 1–8. doi:10.1109/PMAPS.2016.7764155.
- 1062 81. Ailliot, P.; Monbet, V. Markov-switching autoregressive models for wind time series. *Environmental
1063 Modelling & Software* **2012**, *30*, 92 – 101. doi:<https://doi.org/10.1016/j.envsoft.2011.10.011>.
- 1064 82. Pinson, P.; Madsen, H. Adaptive modelling and forecasting of offshore wind power fluctuations with
1065 Markov-switching autoregressive models. *Journal of Forecasting* **2012**, *31*, 281–313. doi:10.1002/for.1194.
- 1066 83. Browell, J.; Drew, D.R.; Philippopoulos, K. Improved very short-term spatio-temporal wind forecasting
1067 using atmospheric regimes. *Wind Energy* **2018**, *21*, 968–979. doi:10.1002/we.2207.
- 1068 84. Browell, J.; Gilbert, C. Cluster-based regime-switching AR for the EEM 2017 Wind Power Forecasting
1069 Competition. 2017 14th International Conference on the European Energy Market (EEM), 2017, pp. 1–6.
1070 doi:10.1109/EEM.2017.7982034.
- 1071 85. Hering, A.S.; Genton, M.G. Powering Up With Space-Time Wind Forecasting. *Journal of the American
1072 Statistical Association* **2010**, *105*, 92–104. doi:10.1198/jasa.2009.ap08117.
- 1073 86. Dowell, J.; Pinson, P. Very-Short-Term Probabilistic Wind Power Forecasts by Sparse Vector Autoregression.
1074 *IEEE Transactions on Smart Grid* **2016**, *7*, 763–770. doi:10.1109/TSG.2015.2424078.
- 1075 87. Messner, J.W.; Pinson, P. Online adaptive lasso estimation in vector autoregressive models
1076 for high dimensional wind power forecasting. *International Journal of Forecasting* **2018**.
1077 doi:<https://doi.org/10.1016/j.ijforecast.2018.02.001>.
- 1078 88. Cavalcante, L.; Bessa, R.J.; Reis, M.; Browell, J. LASSO vector autoregression structures for very short-term
1079 wind power forecasting. *Wind Energy* **2017**, *20*, 657–675. doi:10.1002/we.2029.
- 1080 89. Zhang, Y.; Wang, J.; Wang, X. Review on probabilistic forecasting of wind power generation. *Renewable and
1081 Sustainable Energy Reviews* **2014**, *32*, 255–270. doi:10.1016/j.rser.2014.01.033.
- 1082 90. Dowell, J.; Pinson, P. Very-Short-Term Probabilistic Wind Power Forecasts by Sparse Vector Autoregression.
1083 *IEEE Transactions on Smart Grid* **2016**, *7*, 763–770. doi:10.1109/TSG.2015.2424078.
- 1084 91. Jeon, J.; Taylor, J.W. Using Conditional Kernel Density Estimation for Wind Power Density Forecasting.
1085 *Journal of the American Statistical Association* **2012**, *107*, 66–79. doi:10.1080/01621459.2011.643745.
- 1086 92. Wan, C.; Xu, Z.; Pinson, P.; Dong, Z.Y.; Wong, K.P. Probabilistic Forecasting of Wind Power
1087 Generation Using Extreme Learning Machine. *IEEE Transactions on Power Systems* **2014**, *29*, 1033–1044.
1088 doi:10.1109/TPWRS.2013.2287871.
- 1089 93. Bessa, R.J.; Möhrlen, C.; Fundel, V.; Siefert, M.; Browell, J.; Haglund El Gaidi, S.; Hodge, B.M.; Cali, U.;
1090 Kariniotakis, G. Towards Improved Understanding of the Applicability of Uncertainty Forecasts in the
1091 Electric Power Industry. *Energies* **2017**, *10*. doi:10.3390/en10091402.

- 1092 94. Yıldırım, N.; Uzunoğlu, B., Data Mining via Association Rules for Power Ramps Detected by Clustering or
1093 Optimization. In *Transactions on Computational Science XXVIII: Special Issue on Cyberworlds and Cybersecurity*; Springer Berlin Heidelberg: Berlin, Heidelberg, 2016; pp. 163–176. doi:10.1007/978-3-662-53090-0_9.
- 1094 95. Yıldırım, N.; Uzunoğlu, B. Spatial Clustering for Temporal Power Ramp Balance and Wind Power
1095 Estimation. 2015 Seventh Annual IEEE Green Technologies Conference, 2015, pp. 214–220.
1096 doi:10.1109/GREENTECH.2015.39.
- 1097 96. Yıldırım, N.; Uzunoğlu, B. Association Rules for Clustering Algorithms for Data Mining of Temporal
1098 Power Ramp Balance. 2015 International Conference on Cyberworlds (CW), 2015, pp. 224–228.
1099 doi:10.1109/CW.2015.72.
- 1100 97. Dey, C.H. The Evolution of Objective Analysis Methodology at the National Meteorological Center. *Weather*
1101 and *Forecasting* **1989**, *4*, 297–312. doi:10.1175/1520-0434(1989)004<0297:TEOOAM>2.0.CO;2.
- 1102 98. Ide, K.; Courtier, P.; Ghil, M.; Lorenc, A.C. Unified Notation for Data Assimilation: Operational, Sequential
1103 and Variational. *Journal of the Meteorological Society of Japan. Ser. II, Special Issue on Data Assimilation in*
1104 *Meteorology and Oceanography: Theory and practice* **1997**, *75*, 181–189. doi:10.2151/jmsj1965.75.1B_181.
- 1105 99. Cressman, G.P. An operational objective analysis system. *Monthly Weather Review* **1959**, *87*, 367–374.
1106 doi:10.1175/1520-0493(1959)087<0367:AOOAS>2.0.CO;2.
- 1107 100. Gandin, L., Objective Analysis of meteorological fields; Gidromet, English translation Jerusalem: Israel
1108 program for scientific translation, 1965.
- 1109 101. Kanamitsu, M. Description of the NMC Global Data Assimilation and Forecast System. *Weather and*
1110 *Forecasting* **1989**, *4*, 335–342. doi:10.1175/1520-0434(1989)004<0335:DOTNGD>2.0.CO;2.
- 1111 102. Courtier, P.; Andersson, E.; Heckley, W.; Vasiljevic, D.; Hamrud, M.; Hollingsworth, A.; Rabier, F.;
1112 Fisher, M.; Pailleux, J. The ECMWF implementation of three-dimensional variational assimilation
1113 (3D-Var). I: Formulation. *Quarterly Journal of the Royal Meteorological Society* **1998**, *124*, 1783–1807.
1114 doi:10.1002/qj.49712455002.
- 1115 103. Wu, W.S.; Purser, R.J.; Parrish, D.F. Three-Dimensional Variational Analysis with
1116 Spatially Inhomogeneous Covariances. *Monthly Weather Review* **2002**, *130*, 2905–2916.
1117 doi:10.1175/1520-0493(2002)130<2905:TDVAWS>2.0.CO;2.
- 1118 104. Courtier, P.; Thépaut, J.N.; Hollingsworth, A. A strategy for operational implementation of 4D-Var,
1119 using an incremental approach. *Quarterly Journal of the Royal Meteorological Society* **1994**, *120*, 1367–1387.
1120 doi:10.1002/qj.49712051912.
- 1121 105. Zupanski, D. A General Weak Constraint Applicable to Operational 4DVAR Data Assimilation Systems.
1122 *Monthly Weather Review* **1997**, *125*, 2274–2292. doi:10.1175/1520-0493(1997)125<2274:AGWCAT>2.0.CO;2.
- 1123 106. Evensen, G. Sequential data assimilation with a nonlinear quasi-geostrophic model using Monte Carlo
1124 methods to forecast error statistics. *Journal of Geophysical Research: Oceans* **1994**, *99*, 10143–10162,
1125 [<https://agupubs.onlinelibrary.wiley.com/doi/pdf/10.1029/94JC00572>]. doi:10.1029/94JC00572.
- 1126 107. Turner, M.; Walker, J.; Oke, P. Ensemble member generation for sequential data assimilation. *Remote*
1127 *Sensing of Environment* **2008**, *112*, 1421 – 1433. Remote Sensing Data Assimilation Special Issue,
1128 doi:<https://doi.org/10.1016/j.rse.2007.02.042>.
- 1129 108. Kalman, R.; Bucy, R.S. New Results in Linear Filtering and Prediction Theory. *ASME. J. Basic Eng.* **1961**,
1130 *83*, 95–108. doi:10.1115/1.3658902.
- 1131 109. Jazwinski, A. *Stochastic Processes and Filtering Theory*; Mathematics in Science and Engineering, Elsevier
1132 Science, 1970.
- 1133 110. Ristic, B.; Arulampalm, S.; Gordon, N. *Beyond the Kalman filter: particle filters for tracking applications*; The
1134 Artech House radar library, Artech House, Incorporated, 2004.
- 1135 111. Todling, R.; Cohn, S.E.; Sivakumaran, N.S. Suboptimal Schemes for Retrospective Data Assimilation
1136 Based on the Fixed-Lag Kalman Smoother. *Monthly Weather Review* **1998**, *126*, 2274–2286.
1137 doi:10.1175/1520-0493(1998)126<2274:SSFRDA>2.0.CO;2.
- 1138 112. Anderson, J.L. An Ensemble Adjustment Kalman Filter for Data Assimilation. *Monthly Weather Review*
1139 **2001**, *129*, 2884–2903. doi:10.1175/1520-0493(2001)129<2884:AEAKFF>2.0.CO;2.
- 1140 113. Houtekamer, P.L.; Mitchell, H.L. A Sequential Ensemble Kalman Filter for Atmospheric Data Assimilation.
1141 *Monthly Weather Review* **2001**, *129*, 123–137. doi:10.1175/1520-0493(2001)129<0123:ASEKFF>2.0.CO;2.
- 1142

- 1143 114. Meng, Z.; Zhang, F. Tests of an Ensemble Kalman Filter for Mesoscale and Regional-Scale Data
1144 Assimilation. Part II: Imperfect Model Experiments. *Monthly Weather Review* **2007**, *135*, 1403–1423.
1145 doi:10.1175/MWR3352.1.
- 1146 115. Xiong, X.; Navon, I.M.; Uzunoglu, B. A Note on the Particle Filter with Posterior Gaussian Resampling.
1147 *Tellus A: Dynamic Meteorology and Oceanography* **2006**, *58*, 456–460. doi:10.1111/j.1600-0870.2006.00185.x.
- 1148 116. Uzunoglu, B.; Fletcher, S.J.; Zupanski, M.; Navon, I.M. Adaptive ensemble reduction and inflation.
1149 *Quarterly Journal of the Royal Meteorological Society* **2007**, *133*, 1281–1294. doi:10.1002/qj.96.
- 1150 117. Zupanski, M. Maximum Likelihood Ensemble Filter: Theoretical Aspects. *Monthly Weather Review* **2005**,
1151 *133*, 1710–1726. doi:10.1175/MWR2946.1.
- 1152 118. Houtekamer, P.L.; Mitchell, H.L.; Pellerin, G.; Buehner, M.; Charron, M.; Spacek, L.; Hansen, B. Atmospheric
1153 Data Assimilation with an Ensemble Kalman Filter: Results with Real Observations. *Monthly Weather
1154 Review* **2005**, *133*, 604–620. doi:10.1175/MWR-2864.1.
- 1155 119. Hamill, T.M.; Snyder, C. Using Improved Background-Error Covariances from an Ensemble
1156 Kalman Filter for Adaptive Observations. *Monthly Weather Review* **2002**, *130*, 1552–1572.
1157 doi:10.1175/1520-0493(2002)130<1552:UIBECF>2.0.CO;2.
- 1158 120. Snyder, C.; Zhang, F. Assimilation of Simulated Doppler Radar Observations with an Ensemble Kalman
1159 Filter. *Monthly Weather Review* **2003**, *131*, 1663–1677. doi:10.1175//2555.1.
- 1160 121. Zhang, F.; Snyder, C.; Sun, J. Impacts of Initial Estimate and Observation Availability on Convective-Scale
1161 Data Assimilation with an Ensemble Kalman Filter. *Monthly Weather Review* **2004**, *132*, 1238–1253.
1162 doi:10.1175/1520-0493(2004)132<1238:IOIEAO>2.0.CO;2.
- 1163 122. Möhrlen, C. Uncertainty in wind energy forecasting. PhD thesis, National University of Ireland, Cork,
1164 Ireland, 2004.
- 1165 123. DISPATCH. Technical report, Australiaen Electricity Market Operator (AEMO), Level 22, 530 Collins Street
1166 Melbourne VIC 3000, Australia, 2018.
- 1167 124. Borup, L. IEA Wind Task 36 Forecasting webinar: How to run 40% RE in the Danish system.
1168 <https://www.youtube.com/watch?v=IGhUasWctUM>, last accessed 3. 12. 2018, 2018.
- 1169 125. Germany, B. *EEG in Zahlen* 2016, 2016.

1170 © 2019 by the authors. Submitted to *Energies* for possible open access publication under the terms and conditions
1171 of the Creative Commons Attribution (CC BY) license (<http://creativecommons.org/licenses/by/4.0/>).